

Article

Techno-Economic Optimization of Radiator Configurations in Power Transformer Cooling

Aliihsan Koca ^{1,*}, Oguzkan Senturk ², Ömer Akbal ³ and Hakan Özcan ²

¹ Department of Mechanical Engineering, Faculty of Mechanical Engineering, Istanbul Technical University (ITU), Istanbul 34437, Türkiye

² General Electric Grid Solutions, Gebze 41410, Türkiye; oguzkan.senturk@ge.com (O.S.); hakan.ozcan@ge.com (H.Ö.)

³ Turkish Aerospace Industries, Istanbul 34469, Türkiye

* Correspondence: ihsankoca@hotmail.com or akoca@itu.edu.tr

Abstract: In this research, a numerical approach is created to assess the effective parameters of power transformer thermal management and, as a result, improve their cooling systems. This study analyzes the radiator's thermal performance across several arrangements and optimizes the dimensions and configurations for varied cooling loads from a techno-economic perspective. The optimization criteria were the radiator's height (L), fin spacing (D), and number of fins (N). Due to the great complexity of the generated models, the coupled thermo-hydraulic numerical simulations were carried out on a computer cluster. An in-house radiator test facility was constructed for the experiments in order to verify the numerical model. The simulation findings accord well with the empirically obtained values. A total of 76 radiator sets were investigated. Following that, the generated findings were used to perform an optimization analysis. Finally, the response surface method was used to establish an ideal radiator layout for the specified cooling capacity at the lowest possible cost. These findings reveal that the best cooling performance is obtained when the spacing between the fins is 50 mm. Cooling capacity per unit cost rises as radiator size decreases. The cost factor and geometric details were shown to have strong connections.



Citation: Koca, A.; Senturk, O.; Akbal, Ö.; Özcan, H. Techno-Economic Optimization of Radiator Configurations in Power Transformer Cooling. *Designs* **2024**, *8*, 15. <https://doi.org/10.3390/designs8010015>

Academic Editor: Xiaohu Yang

Received: 24 December 2023

Revised: 28 January 2024

Accepted: 30 January 2024

Published: 2 February 2024



Copyright: © 2024 by the authors. Licensee MDPI, Basel, Switzerland. This article is an open access article distributed under the terms and conditions of the Creative Commons Attribution (CC BY) license (<https://creativecommons.org/licenses/by/4.0/>).

Keywords: power transformer; computational fluid dynamics; ONAN; transformer cooling; thermal–economical assessment

1. Introduction

Oil-immersed power transformers are widely recognized as highly valuable components within electrical power networks. During the process of converting electric energy from high to low voltages, some of the energy is dissipated as heat, which occurs in the windings, core, and structural components. During the process of converting electric energy from high to low voltages, some of the energy is dissipated as heat, which occurs in the windings, core, and structural components. This heat must be efficiently dissipated by the cooling system. Although the majority of this heat is extracted from the radiators, a portion of it is also extracted from the oil tanks. The dissipation of heat from the windings and core is facilitated by the circulation of oil, which traverses the spaces between the winding disks. Subsequently, the oil flows through the upper pipes of the radiators, transferring the heat to the cooling channels within the fins. Eventually, the oil reaches the lower pipes of the radiators before returning to the windings at the bottom. There are four primary cooling modes employed in transformers: oil-natural air-natural (ONAN), oil-natural air-forced (ONAF), oil-directed air-forced (ODAF), and oil-forced air-forced (OFAF). Non-direct oil flow cooling systems, such as ONAN, are widely employed in power transformers due to their high reliability. The circulation of oil through the flow system is primarily driven by thermal forces resulting from variations in oil density [1].

In the context of ONAN-cooled power transformers, the circulation of oil through the cooling network and the movement of air through the radiator fins are driven by natural convection resulting from buoyancy effects. A comprehensive understanding of the principles governing the flow of heat and dissipation in radiators is of the utmost significance for transformer manufacturers. The determination of the design parameters that can influence the heat dissipation process of radiators and enable the enhancement of design also draws attention within the transformer business. A more efficient design allows for a reduction in the size and the weight of the radiator, resulting in improved efficiency, extended lifespan, and decreased manufacturing costs, all while effectively dissipating a given amount of heat. Due to this rationale, the manufacturers of transformers exhibit a strong inclination towards minimizing the quantity of radiator with the objective of reducing the overall weight of the system, while ensuring that the thermal performance remains uncompromised. Additionally, improved radiator thermal performance may also reduce the weight of the active part components.

The main goals of this research are to investigate the radiator's thermal performance in a range of dimensions and configurations and to optimize those dimensions and configurations for a variety of cooling loads from a techno-economic standpoint. The optimization parameters are the radiator height, the fin spacing, and the number of fins in a radiator.

The majority of the existing literature focuses on the internal cooling mechanisms employed in power transformers, specifically pertaining to the cooling of the windings. In contrast, the process of externally cooling the transformer, specifically through the utilization of radiators, involves significantly less effort. The absence of significant cooling issues in power transformers in the past can be attributed to the design of their cooling systems, which incorporated an excess number of radiators beyond the actual cooling requirements of the transformers [2]. Considerable efforts have been undertaken in recent times to decrease the dimensions and quantity of radiators employed for the purpose of cooling power transformers. This endeavor aims to mitigate the escalating production costs resulting from the surge in raw material prices and the trend towards downsizing power transformers. In order to achieve an optimal cooling system for power transformers, it is imperative to conduct studies on the design of a radiator that exhibits superior performance.

Considering the advent of sophisticated tools like computational fluid dynamics (CFD), it has become feasible in recent years to virtually visualize the airflow and temperature distribution across radiators, thereby eliminating the need for costly experimental procedures. In addition, the analysis of air-flow distribution provides further understanding and potential avenues for enhancing the thermal efficiency of the system. By employing numerical methods, it becomes feasible to compute the heat losses and variation in temperature in power transformers and systems for cooling [3,4]. Nevertheless, the numerical challenges encountered in natural convection problems include issues related to convergence, computational time, and accuracy [5,6].

In their research, Fdhila et al. [7] investigated the heat transfer phenomenon in air-cooled radiators with a large size. They employed a CFD model to simulate the heat transfer process, considering the combined effects of oil and air flows through mixed convection. The heat transfer between these two media within the radiators was modeled using an anisotropic porous medium approach. Additionally, the surrounding area of the radiators was modeled using a standard turbulent heat transfer model. The authors introduced a rapid and precise methodology for conducting simulations pertaining to a significant category of radiator cooling issues. Kim et al. [8] conducted an investigation into the cooling efficiency of radiators utilized in oil-filled power transformers, specifically focusing on the application of ONAN and ODAN. The study employed analytical, numerical, and experimental methods to analyze the cooling performance of these radiators. The researchers conducted an analytical prediction of the temperature distribution and cooling performance of the radiator, which was subsequently validated using CFD results. Cha et al. [9] investigated the influence of thermal head on the flow rate of an insulating oil in the pathway between a transformer and a radiator. The researchers employed com-

mercial CFD software to conduct their analysis. It was discovered that the flow rate of the insulating oil exhibited an increase in correlation with the thermal head, consequently leading to an enhancement in the cooling efficiency of the radiator. Tălu and Tălu [10] conducted a study on the cooling efficiency of a 630 kVA transformer radiator. This investigation employed numerical analysis techniques, specifically utilizing the Finite Element Method (FEM). The researchers examined the cooling efficiency of the radiator based on the ambient air temperature surrounding the radiator. Hence, it has been verified that the cooling efficiency of the radiator is enhanced when the angle of inclination throughout the cooling manifold and the transformer is approximately 20 °C.

Seong et al. [11] conducted a numerical investigation to analyze the fluid flow and heat transfer distribution within a transformer radiator. This analysis was performed using commercially available CFD software. The researchers conducted an analysis on the cooling efficiency of the radiator by employing various cooling techniques. The researchers discovered that augmenting the overall length of the radiator yielded better results in enhancing the cooling efficiency, as opposed to increasing the quantity of radiator fins.

Dorella et al. [12] utilized computational fluid dynamics (CFD) simulations to conduct the thermal design of a power transformer radiator. The analysis of thermo-fluid dynamic performance was conducted by introducing artificial body forces and a numerical scheme. Turbulators and wall indentation arrangements were proposed to improve heat transfer and increase cooling capacity. Simulations demonstrated that these modifications enhance the heat transfer coefficient and the cooling capacity of the radiator. Azbar et al. [13] conducted a study. A 3D numerical simulation was conducted to investigate the impact of geometrical and operational parameters on the cooling of three-phase power transmission transformers. The study investigated the morphology of transformers, including their shape, fin shape, and arrangement. Circular and hexagonal shapes, when compared with traditional transformer shapes, resulted in a decrease in average oil temperature. The unequal heights of the fins enhanced the cooling process. The trapezoidal perforated fins exhibited the highest thermal performance. The hexagonal transformer, equipped with a perforated trapezoidal fin, achieved a 12% greater reduction in oil compared with the rectangular transformer.

In their study, Cho and Kim [14] introduced a computational approach for determining the cooling efficiency of radiators employed in power transformer cooling systems. They utilized two well-established models to address the heat transfer resulting from natural convection within the radiator and the surrounding cooling air. A comparative analysis was conducted between the outcomes derived from two conventional models and the results obtained through CFD analysis, as well as the experimental data. The objective of this investigation was to gain insights into the heat transfer mechanisms occurring within the radiator and to develop an optimal cooling system for power transformers. In a similar vein, Shim et al. [15] conducted a numerical analysis to investigate the natural convection occurring between the radiator and the surrounding cooling air. The study employed a simplified mathematical model for this purpose. In addition, a CFD analysis was conducted to examine the fluid flow and heat transfer phenomena surrounding both the actual and simplified configurations of a radiator, as influenced by natural convection. The researchers conducted a comparison between their CFD findings and the outcomes derived from the simplified mathematical model, as well as the experimental data. Nabati et al. [16] conducted numerical simulations to analyze the variation in temperature and flow distribution within a radiator used for ONAN cooling. The primary objective of their research was to investigate the correlation between the characteristics of the radiator and the cooling performance of the system.

Rodriguez et al. [17] presented a comprehensive study on a conventional 30 MVA power transformer, encompassing semi-analytical calculations, CFD simulations, and experimental measurements. The analysis focused on the capacity for cooling of the current radiator development when operating in ONAN mode, with a brief discussion of potential enhancements to the existing design. The creation of a thermo-hydraulic radiator model that

accurately predicts oil temperatures and is applicable to various types of oils was described by Van der Veken et al. [18]. This model was based on physical equations. The authors of the study introduced a methodology to estimate airflow velocity by considering the fan properties and radiator structure in thermal calculations. In their study, Chandak et al. [19] conducted a numerical analysis to investigate the impact of radiation on the transfer of heat from a transformer radiator. The researchers observed that a consideration of radiation is necessary when examining the natural convection scenario. With the exception of the studies conducted by Paramane et al. [20] and Van der Veken et al. [18], the aforementioned numerical investigations did not take into account radiation heat transfer.

Medeiros et al. [21] performed a thermal experimental assessment of a power transformer under the cooling conditions of oil-directed (OD), oil-forced (OF), and oil-natural (ON). In order to ensure safe functioning, it is important to design a cooling system that can effectively regulate the transfer of heat to the surrounding environment. Their study investigated the thermal efficiency of a prototype transformer using three different cooling methods, offering significant insights for the development of dependable transformer designs. The ON mode offers higher temperatures at a lower cost and maintenance level. However, achieving better thermal performance requires the use of external pumps, which incur additional costs. Rodrigues et al. [22] evaluated the thermal efficiency of power transformers and the placement of optical fiber sensors for temperature monitoring. The article employed an experimental and computationally combined method to examine the thermal performance of power transformers and assess the positioning of optical sensors. The study involved comparing measurements obtained from a prototype power transformer with 20 optical fiber sensors to CFD simulations. The study demonstrated that temperature measurements obtained at certain times may not accurately depict the critical temperatures along the windings of transformers.

The existing literature contains studies that investigate the impact of geometric parameters on cooling performance and explore geometric optimization for transformer-cooling systems from a thermal perspective. In their study, Raeisian et al. [23] conducted a CFD analysis on a 200 kVA distribution transformer operating under the ONAN-cooling regime. The researchers focused on identifying the key geometric parameters that have the most significant impact on the hotspot temperature. The present study employed a response surface methodology to optimize the radiator's geometry. Amoiralis et al. [24] conducted a numerical investigation on the optimal design of the ONAN transformer-cooling apparatus. The study investigated various tank designs for transformers, considering additional important factors such as the quantity and placement of the winding cooling ducts. The objective was to analyze how the geometry of the tank influences the performance of the cooling system in transformers. The cooling effectiveness of a power transformer with ONAN cooling was numerically investigated by Anishek et al. [25], although experimental validation was not conducted. An optimization analysis was conducted on the radiator, revealing that the proposed design exhibited a 14% improvement in cooling performance compared with an existing design, while maintaining the same material cost. The researchers conducted a study to examine the independent impact of radiator height and fin spacing on cooling performance. In a study conducted by Smolka [26], the utilization of CFD and genetic algorithm techniques was employed to propose an optimal arrangement for the windings and associated oil channels. The objective of this configuration was to effectively reduce the temperature of hotspots within the winding system. In their study, El Wakil et al. [27] utilized a numerical approach to investigate the heat transfer and fluid flow characteristics of an insulating medium within one phase of a three-phase 40 MVA power transformer. It is important to note that the numerical method employed by the authors was not validated through experimental means. The researchers examined six distinct geometrical configurations and six varying oil flow rates to analyze the impact of these parameters on the cooling efficiency. Chereches et al. [28] conducted a numerical parametric analysis on a modified power transformer in order to examine the impact of different parameters on the cooling system's performance. According to their findings, the placement of an

obstacle at the lower section of the transformer facilitated the directed flow of coolant towards the region with the highest temperature, resulting in a reduction of the maximum temperature. Nematzadeh et al. [29] introduced two innovative integrated power cycles designed specifically for low-temperature heat sources. This was demonstrated through a thorough thermoeconomic simulation of the system. According to the findings, the throttle valve and absorber are the most detrimental components. An analysis of crucial parameters indicated that the generator and condenser temperatures have a direct impact on the energetic efficiency of the proposed power cycles, causing them to either increase or decrease. In their study, Eslamian et al. [30] utilized FEM and CFD approaches to simulate the heat transmission of a dry-type transformer. They examined the impact of various factors, including duct width, on the temperature distribution within the transformers.

A comprehensive review of the existing literature reveals that while a considerable amount of research has been conducted on the cooling systems of transformers, the process of optimizing these systems is still in its nascent phase. The optimization efforts can be classified into two primary groups based on the methodology employed in the investigation. The first group has focused on examining the impact of different geometrical parameters on the hotspot temperature in windings, as evidenced by references [23,25,28,30]. The second group has worked on studying the effects of a variety of geometrical parameters on the total cooling performance of the transformer cooling system, as indicated by references [24,25,27]. The verification experiments were carried out in a limited number of optimization studies, specifically [23,26,30]. Furthermore, none of the aforementioned studies have taken into account an optimization study from an economic perspective. In this study, for the first time, optimal radiator configurations from both thermal and economic perspectives, with the goal of reducing investment costs, have been investigated.

The main aims of this study are to investigate the thermal effectiveness of the radiator under different configurations and dimensions and to optimize these dimensions and configurations based on a techno-economic analysis for varying cooling loads. Within the confines of this specific context, the optimization criteria were determined to be the height of the radiator (L), the spacing between radiator fins (D), and the quantity of fins (N) contained within a radiator. Given these objectives, the cost factor is also examined. The results obtained from this extensive analysis provide significant contributions to the field of heat transfer optimization. Through the acknowledgment of the robust association between geometrical variables and heat transfer, coupled with the concurrent consideration of cost implications, individuals engaged in research, engineering, and practical applications can make well-informed choices when designing or optimizing systems to achieve improved thermal efficacy and cost-effectiveness. Hence, this study presents radiator geometric configurations that offer the most cost-effective solutions for achieving the desired cooling capacities. The aforementioned objectives were successfully accomplished through the implementation of the subsequent measures. The simulation of the flow and temperature fields within the radiator, as well as the surrounding ambient air and solid components, was conducted using Ansys Fluent 2023 R1[®] software, a widely used commercial CFD tool. Furthermore, the numerical model was verified using experimental data. Subsequently, a numerical investigation was conducted to examine the effects of various geometrical parameters. Finally, the response surface method (RSM) was employed, utilizing the commercially available statistical software, MINITAB v19[®], to attain an optimal arrangement of the radiator that ensures the desired cooling capacity while minimizing associated costs. It should be noted that this research used a transformer cooling system based on the ONAN mode, thereby limiting the applicability of the findings to other cooling modes.

Since the modeling of the air and oil domains is expensive, the majority of numerical studies do not take radiation heat transfer into account, with the exception of Paramane et al. [2,20] and Van der Veken et al. [18]. Hence, an additional innovation of this study involves the incorporation of modeling for both fluid and solid domains, as well as radiation heat transfer within the air domain, in order to achieve comprehensive and accurate simulations. The simulations were conducted using a high-performance computing system

comprising 500 processors. Previous research has shown that there is a disparity between the number of experimental investigations and numerical studies conducted. Hence, an additional aim of this study is to present supplementary data from experiments in order to enhance comprehension of the thermal properties of transformer cooling systems. In order to obtain precise test results for different transformer cooling applications in diverse climatic conditions, a comprehensive experimental setup was meticulously designed and constructed. The experimental studies were conducted at the facilities of the General Electric Grid Solutions company. Figure 1 shows the schematic illustration of this study.

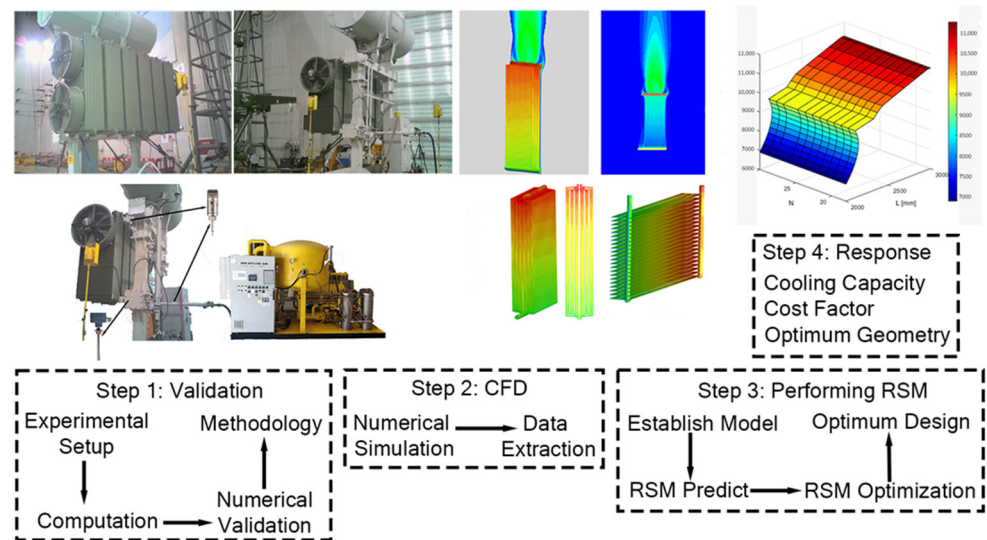


Figure 1. Schematic illustration of the study.

2. Numerical Methodology

The cooling model considered in the current cooling system is the AN (air-natural) model. In the AN-cooling model, the radiators are cooled through natural convection, whereby cooling fans are absent and heat dissipation occurs solely along the surface of the radiators. The transformer under consideration employs mineral oil as a circulating cooling medium within both the active part and the tank. This facilitates the absorption of heat from the core and windings, which is subsequently dissipated to the surrounding air through the tank and fin surfaces. The purpose of this cooling system is to ensure a consistent and dependable temperature distribution throughout the transformer. In this context, the oil contained within the transformer was regarded as the numerical domain, and its convective heat transfer was modeled and simulated in a 3D manner. To obtain a comprehensive understanding of the fluid dynamics within the radiator, as well as the associated temperature distribution and heat transfer, a numerical model was developed.

The primary objectives of this simulation study are to examine the thermal performance of the radiator across various configurations and dimensions, as well as to optimize the dimensions and configurations from a techno-economic perspective for different cooling loads. In the present context, the optimization criteria encompass the determination of the radiator height, the spacing between the fins, and the quantity of fins within a radiator. The evaluation of these three parameters is necessary as they are interdependent criteria that should be considered in conjunction. In this context, the simulations were categorized into two distinct components. The investigation focused on determining the gap between each fin. Furthermore, an examination was conducted on the height and quantity of radiator fins. A total of 76 sets of radiator configurations were examined. The input data for the techno-economic study are derived from the results obtained through CFD simulations.

2.1. Physical Model

Radiators are heat exchangers made of steel plates that are typically positioned in a vertical orientation mounted on transformers. The panels comprise two steel fins that are pressed and welded together. In the context of simulation studies, a solitary radiator is represented as a physical model. Given the large number of elements and the significant computational load, the utilization of the symmetry boundary condition is employed. The CAD model was generated using CATIA V5R28[®] software and parametrically prepared utilizing the Design Table[®] feature. In a solid modeler, the process of geometry clean-up involves the removal of brackets and other small components. This procedure does not have a substantial impact on flow and heat transfer. Additionally, this approach contributed to a reduction in the duration needed for meshing, consequently resulting in decreased computational time. Figure 2 displays the visual representation of the CAD geometry with dimensions after undergoing the cleaning process. The vertical attachment of panels with a standardized width of 520 mm and varying heights ranging from 1000 to 3000 mm can be observed in the frontal view of the diagram. These panels were affixed to the horizontal header pipe. This study examines a range of 11–35 fins per radiator, which were horizontally positioned with inter-finned gaps measuring 35–50 mm. The hot oil was introduced into the upper collectors, where it traversed through these channels. During this process, thermal energy was transferred from the oil to the steel fin, subsequently dissipating into the air that circulates between the radiator fins. Ultimately, the downward movement of oil within the radiator fins was subjected to cooling, subsequently entering the lower header pipe and returning to the transformer tank. The sizing and design processes for transformer radiators are described in detail in the Appendix A.

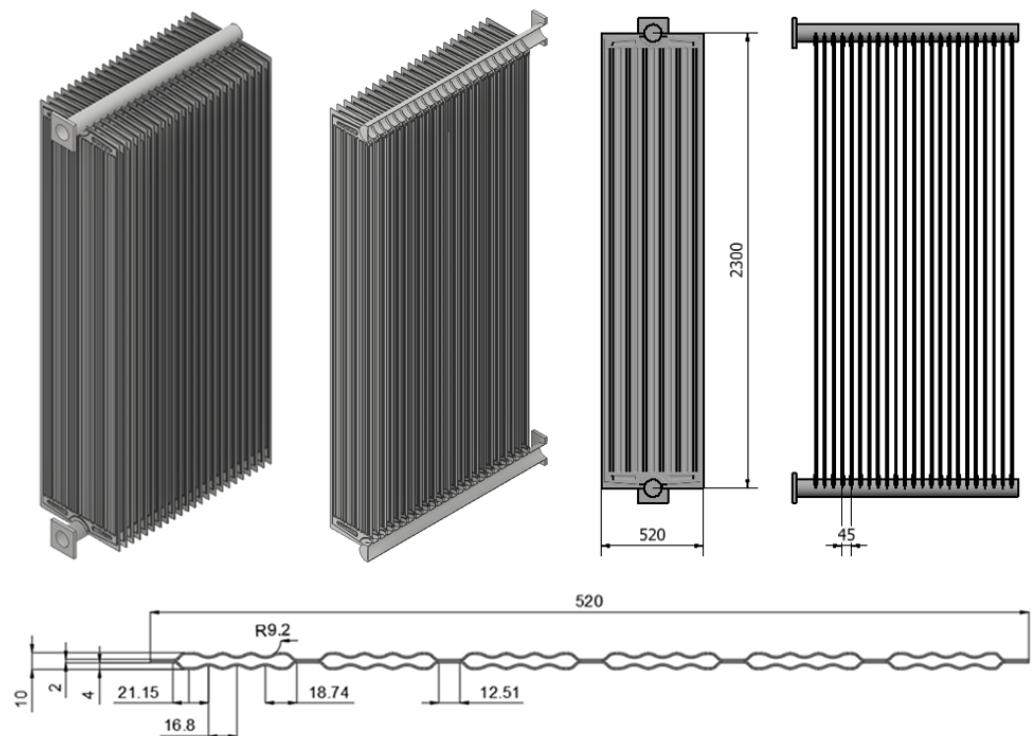


Figure 2. Dimensions of the radiator.

In order to mitigate the entrance effect and minimize the backflow resulting from the wake, the lengths of both the inlet and outlet pipes were extended. According to the details presented in Figure 3, the radiator consisted of upper and lower manifolds with a diameter of 88.9 mm. Additionally, each individual radiator fin had a width of 520 mm. Once the geometries were simplified, the flow volume for the fluid (oil) was generated. The simulations did not incorporate the volumetric representation of the radiator slice. The

high thermal conductivity of the metal material used in the radiator slice with a thin wall thickness allowed for the neglect of heat conduction resistances within the wall thickness. The volume of oil extracted for the solid volume and final domain was determined, as depicted in Figure 3. Subsequently, in order to assess the impacts of natural convection, air domains of considerable size were generated, originating from and extending beyond the edges of the radiator. The air inlet is defined as a pressure inlet from all sides, while the air outlet is defined as a pressure outlet located at the top. The 'Wall' boundary condition was specifically designated for the ground surface.

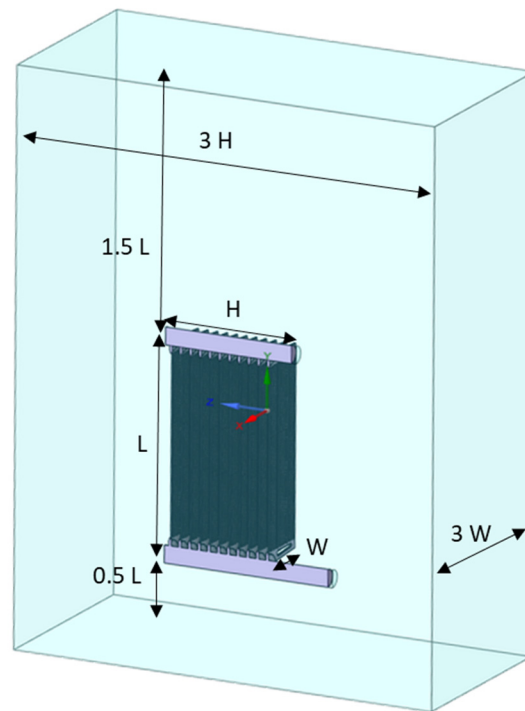


Figure 3. The computational domain.

2.2. Grid Generation

The Fluent T-Grid Mesher[®] was employed to generate the grid for both models due to its flexibility and ability to regulate grid quality and optimize grid density during the grid production process. Subsequently, the grid configuration for each subdomain was established through the implementation of various localized procedures. Given the significant variation in dimensions, particularly for the radiator fins with a height of 3 m and a fin thickness of 1 mm, the geometry in this study was subjected to simplification to minimize its impact on the outcomes of the real system. The control of mesh quality in different regions of the domain was achieved through the utilization of various options available in the software. The mesh structure of choice was poly-hexcore. The poly-hexcore mesh structure employs polyhedral elements in close proximity to the wall, while hexagonal elements are utilized in regions further away from the wall. Hence, as depicted in Figure 4, all surface meshes exhibited a polyhedral configuration and employed a hexagonal mesh pattern within the flow region. The poly-hexcore structure exhibited reduced memory coverage properties and a lower element count compared with solution meshes featuring a tetrahedral or polyhedral structure. Consequently, the utilization of a poly-hexcore structure led to a reduced analysis time while simultaneously achieving a higher-quality mesh. If the standard tetrahedral mesh was employed, there would be a sixfold increase in the total number of meshes and the corresponding resolution times.

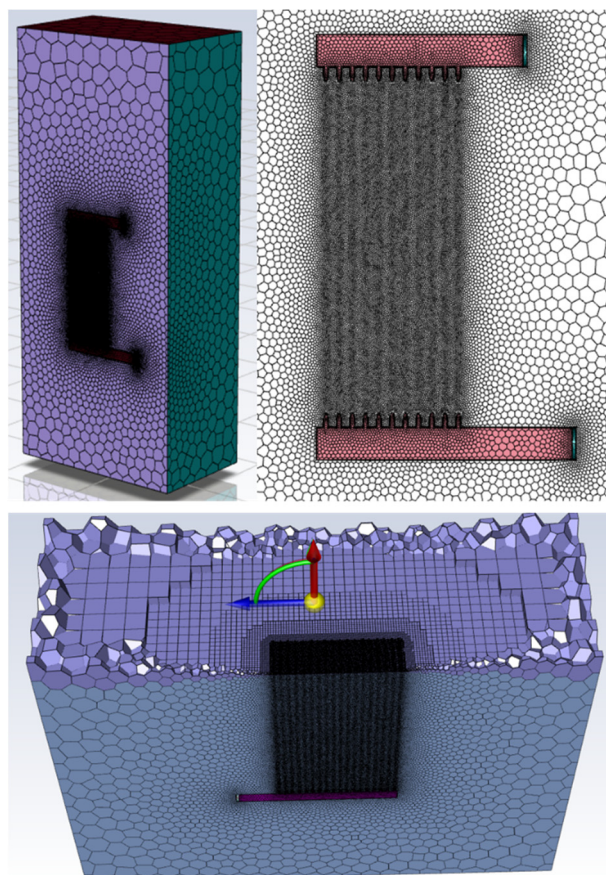


Figure 4. The surface mesh and volume grid structure.

A grid independence analysis was conducted for both models in order to determine the most suitable grid size for numerical calculations. A mesh independence analysis was conducted on the radiator geometry, which had a length of 2300 mm and 23 fins. Initially, the geometry files were transferred to the Fluent Meshing[®] platform, where a surface mesh was generated. Subsequently, a volume mesh was acquired. Four grid structures were generated and analyzed under identical boundary conditions in this study. The grid densities employed for the simulations of heat transfer and fluid flow in the selected models varied within the range of 16 to 36 million. The primary criterion for independence was the average temperature of the oil upon exiting the radiator. The temperatures were selected as parameters to assess the outcomes of the energy solution model, while the velocity values were chosen as parameters to evaluate the outcomes of the flow (turbulence) solution model.

Figure 5 depicts the computed oil outlet temperatures ($T_{oil,out}$) for each of the grid structures. The difference in oil outlet temperature between the Grid-3 and Grid-4 grid configurations is less than 1%, as shown in Table 1. Based on the results obtained, it can be observed that the oil outlet temperatures, which can be considered as a measure of overall heat transfer quantities, tend to stabilize at consistent levels as the grid resolution is increased (see Figure 5). The findings of this study indicate that grid structures containing approximately 24 million cells exhibit sufficient precision in capturing the thermal and hydrodynamic boundary layers in close proximity to the critical surfaces. The grid structures were employed in all the simulations by modifying them parametrically based on the dimensions of the model. The investigation of independence was conducted on the smallest radiator, resulting in larger geometries containing over 100 million elements. This is indicative of a significant amount of time dedicated to calculations.

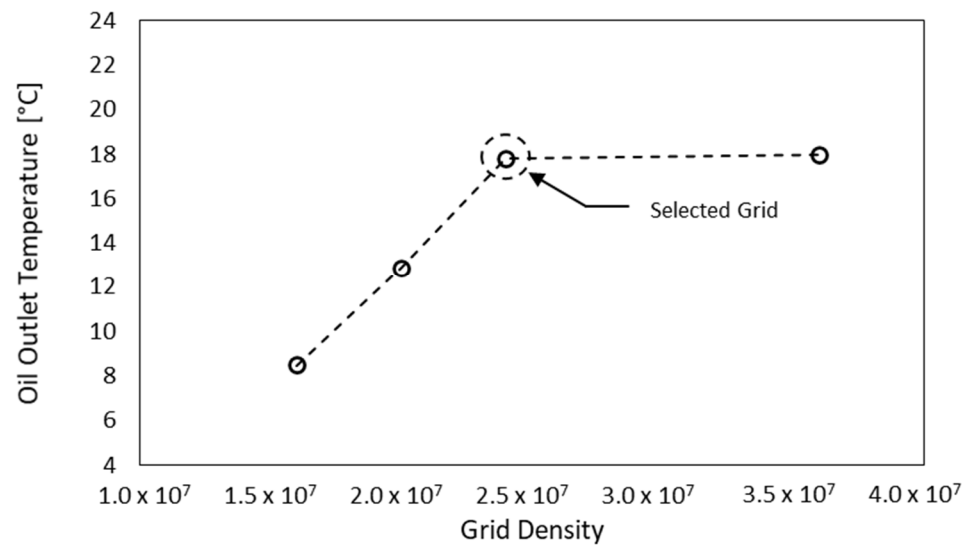


Figure 5. Grid independency results.

Table 1. Results of different mesh densities.

Parameter	Grid Density	Oil Inlet Temperature ($T_{oil,in}$) [°C]	Oil Outlet Temperature ($T_{oil,out}$) [°C]	Average Air Velocity (V_a) [m/s]
Grid-1	~16 million	54.6	8.45	0.23338
Grid-2	~20 million	54.6	12.85	0.23299
Grid-3	~24 million	54.6	17.80	0.23152
Grid-4	~36 million	54.6	17.95	0.23165

In order to increase the precision of velocity and temperature gradient measurements in the near-wall regions, the grid element size was decreased as it approached the heat transfer surfaces. By employing this approach, the gradient near the wall was accurately resolved in order to effectively capture the boundary layer phenomenon. The investigation also included an examination of the non-dimensional wall distance parameter (y^+), which plays a significant role in the adjustment of fluid shear stress and heat transfer near the wall. This parameter defines the region of the wall law where the governing equations are solved. During the process of dimensioning the boundary layer of the solution grid, the k-w SST turbulence model was formulated with the objective of maintaining the y^+ parameter at a value below 1. The requisite computations were conducted by employing established turbulent boundary layer equations for a planar surface, as documented in relevant research papers. To determine the initial grid point, a target y^+ value of less than 1 was taken into account. The first cell height was then computed as 0.2 mm for oil domains and 0.15 mm for air domains. In this particular context, an investigation was conducted to assess the influence of the number of boundary layer meshes in proximity to heat transfer surfaces on cooling effectiveness. This was achieved by employing various boundary layer mesh sizes and stretching ratios. The results indicate that there was a decrease of 0.1% in the overall cooling capacity when the density of the mesh at the surface was increased. This suggests that the impact of the boundary layer on the accuracy of the simulation outcomes is insignificant, affirming the suitability of the chosen boundary layer thickness. In order to avoid encountering any divergence issues, a maximum skewness value of 0.815 was maintained for all models within the selected mesh configuration. The properties of the chosen grid configuration are presented in figures provided herein.

A close up view near the heat transfer surfaces of the radiator is shown in Figure 6.

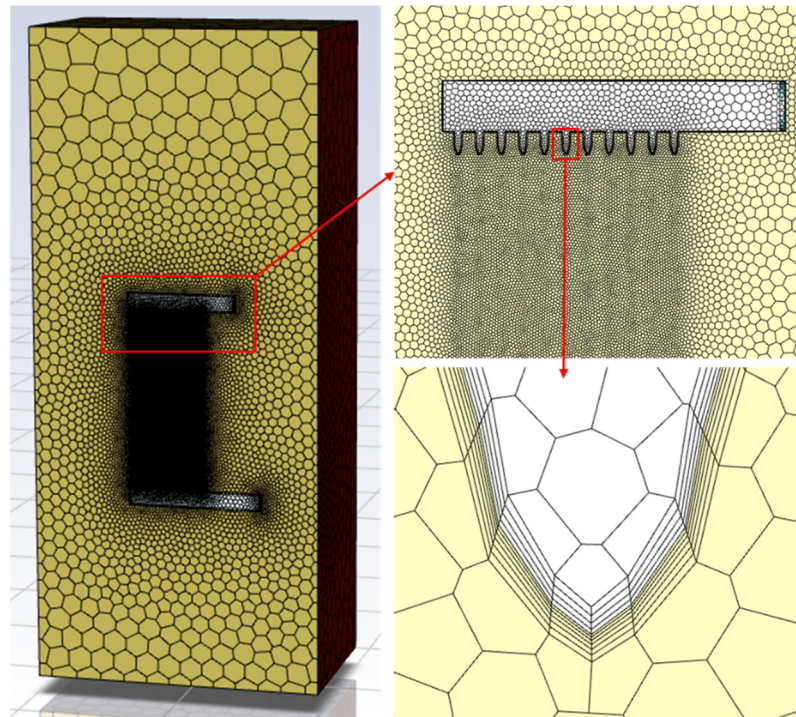


Figure 6. Isometric and section views of the grid structures.

2.3. Solution Methodology and Boundary Conditions

The simulations were conducted on a high-performance computing system comprising 500 processors. The time needed to complete a single simulation on 500 processors was approximately 8 h, resulting in a total computing time of approximately 200,000 CPU-hours. This significant amount of computing time was primarily due to the inclusion of modeling for fluid and solid domains, as well as radiation heat transfer in the air domain. The equations governing the conservation of mass, momentum, and energy for the fluid (oil and air) inside and outside the radiator can be denoted as Equations (1)–(3). These equations describe the three-dimensional, incompressible, and turbulent flow of the fluid, as well as the heat transfer, in the radiator of the transformer for the current conjugate heat transfer and fluid flow problem. The equation representing the conservation of energy for the conduction of heat transfer in the solid component of a radiator can be denoted as Equation (4).

$$\frac{\partial(\rho u_i)}{\partial x_i} = 0 \tag{1}$$

$$\frac{\partial(\rho u_i u_j)}{\partial x_i} = -\frac{\partial P}{\partial x_j} + \frac{\partial}{\partial x_i} \left(\mu \frac{\partial u_j}{\partial x_i} - \rho \overline{u_i' u_j'} \right) + \rho g_j \beta (T - T_a) \tag{2}$$

$$\frac{\partial(\rho u_i T)}{\partial x_i} = \frac{\partial}{\partial x_i} \left(\frac{k_f}{c_{p,f}} \frac{\partial T}{\partial x_i} - \rho \overline{u_i' T'} \right) \tag{3}$$

$$\frac{\partial}{\partial x_i} \left(k_s \frac{\partial T}{\partial x_i} \right) = 0 \tag{4}$$

Equations (1)–(3) correspond to the conservation principles for the mass, momentum, and energy of the fluid (either oil or air) inside and outside the radiator. In this context, the symbols u , P , T , and x in Equations (1)–(4) correspond to the variables representing velocity, pressure, temperature, and coordinate direction, respectively. The symbols T_a , β , μ , ρ , k_s , k_f , and $C_{p,f}$ denote the surrounding ambient air temperature, the thermal expansion coefficient of air, the viscosity of the fluid, the density of the fluid (either oil or air), the thermal conductivity of the solid (stainless steel), the thermal conductivity of

the fluid, and the specific heat of the fluid, respectively. The terms $-\overline{\rho u_i' u_j'}$ and $-\overline{\rho u_i' T'}$ in the given context denote the Reynolds stress and turbulent heat flux, respectively. The variable $\rho g_j \beta (T - T_a)$ denotes the buoyancy term associated with the surrounding cooling air, as defined by the Boussinesq approximation. The utilization of subscripts i and j within the equations denotes the application of tensor notation. The application of the finite volume method was employed to discretize and assess the boundary conditions as well as the three-dimensional governing equations on a computational grid. The control volume technique involves integrating the internal conservation equations of each control volume and implementing discrete formulations that maintain relevant values [31,32]. The development of a segregated solver with double-precision was undertaken with the aim of solving the Navier–Stokes equation. The resolution of the interaction between pressure and velocity was achieved through the utilization of the PRESTO algorithm, which is compatible with the Boussinesq approach. The Fluent software's shell conduction method was employed to compute the conductive heat transfer occurring within the radiator fins. The utilization of the Boussinesq approach was employed in order to enhance the accuracy of modeling the buoyancy effects associated with natural convection. This approach yielded superior precision outcomes at a reduced computational expense for fluid motions characterized by small variations in density, such as those observed in natural convection. The investigation of the proposed enhancement in wall treatment by Menter [33] was conducted utilizing the shear stress transport (SST) κ - ω turbulence model. The SST κ - ω turbulence model has been found to exhibit a high level of accuracy and dependability. It is capable of evaluating distinct flows and adverse pressure variations by employing the κ - ω model in proximity to wall surfaces and the κ - ω model in the primary flow region [33]. The surface to surface (S2S) radiation model was utilized to simulate the heat transfer of surface radiation in various radiator configurations. In this model, an emissivity value of 0.95 was assigned to the radiator surface.

The diffusion component in the momentum and energy equations was evaluated using a second-order central difference method, resulting in a trustworthy outcome. The utilization of the least squares cell-based technique, which has been proven to be efficient in scenarios where highly skewed cells are present within the calculation domain, was employed to discretize the spatial gradients. In order to ensure convergence during the computations, under-relaxation factors of 0.50, 0.25, 0.75, and 0.50 were specified for momentum, pressure, turbulence, and energy, respectively. In the context of a steady-state computational fluid dynamics analysis, a convergence threshold of 10^{-6} was selected to assess the convergence of the continuity, energy, and momentum variables. Additionally, discrepancies in the mass flow rate were observed, prompting the execution of iterative processes to minimize these imbalances to a satisfactory threshold of less than 0.3%. The temperature of the output oil, weighted by its mass, was also monitored during the iterations. Once the outlet temperature was established within a stable range, the calculations were carried out until the desired residuals were achieved.

Subsequently, the implementation of hybrid initialization was initiated, followed by the execution of various assessments. The radiation model was not activated during the initial 2000 iterations of the analysis. Once the convergence results had reached the desired levels, the radiation model was subsequently activated, and an additional 4000 iterations were executed. After undergoing 6000 iterations, the temperature monitoring point exhibited a deviation of merely 0.02% from its ultimate value. The energy balance was carefully maintained in each simulation, ensuring that the net heat transfer rate between the inflow and outflow heat transfer surfaces differed by less than 0.1%.

Boundary conditions were defined using data obtained from thermal tests conducted in the experiment. The boundary conditions at the inlet of the radiator for the internal flow of oil included an experimentally determined mass flow rate of 0.250 kg/s, an average inlet temperature of $T_{in,ave} = 54.6$ °C, a turbulence density of 1%, and a hydraulic diameter of 0.0889 m. An outlet boundary condition was implemented at the outlet, where the average static pressure was prescribed as 0 Pa. The aforementioned boundary condition was

employed in situations where the flow was primarily oriented towards the exterior of the domain. In the context of external air flow, it is conventionally accepted that the reference ambient temperature is denoted as $T_a = 15\text{ }^\circ\text{C}$. No boundary criteria for the heat-transfer faces are specified by the user. This phenomenon arises from the interconnectedness of heat transfer surfaces, wherein a solid zone is juxtaposed with a fluid zone on the opposing side. To ensure that each side of the wall corresponds to a physical wall, the solver employs an automated process to create a designated region called “shadow” when a grid containing a connected wall of this nature is imported. Consequently, by utilizing the information contained within the adjacent cells, it is possible to directly calculate the heat transfer. The side walls of the structure are classified as opening boundaries, facilitating the unobstructed movement of air in these areas. In contrast, the ground functions as a no-slip wall, impeding the flow of air. The opening boundary condition was specified to have a very low intensity of turbulence, specifically at a level of 1%. The rationale behind utilizing a low turbulence intensity is attributed to the phenomenon of air being drawn and expelled into an environment that is characterized by a state of relative quiescence. It is necessary to acknowledge that stainless steel, a material with consistent properties, was specifically designated for solid components. These properties include a density (ρ) of 8030 kg/m^3 , a specific heat capacity (c_p) of 502.48 J/kg K , and a thermal conductivity (k_f) of 16.27 W/mK . Mineral oil, when utilized as a refrigerant, is a distinct type of oil. The thermophysical characteristics of this oil were derived from prior investigations conducted by the GE Company. The simulation program incorporated the temperature-dependent thermophysical properties of mineral oil. Regarding the air properties, the density of the air in the vicinity of the radiator fin is described by the Boussinesq equations. Based on our preliminary simulation studies, we found that the radiator’s surrounding air temperature varies within a small range ($20\text{ }^\circ\text{C}$ to $30\text{ }^\circ\text{C}$). Therefore, the air’s thermophysical properties were assumed to be constant since its final results would not be significantly altered. The characteristics of air were evaluated under standard conditions of 1 Atm of pressure and a temperature of $25\text{ }^\circ\text{C}$. It is postulated that the thermophysical properties of the air remain constant regardless of temperature, with $c_p = 1006\text{ J/kg K}$, $k_s = 0.02437\text{ W/mK}$, $\mu = 1.78 \times 10^{-5}\text{ kg/m.s}$, and $\beta = 0.00312\text{ K}^{-1}$.

3. Validation Study

In order to ascertain the precision of numerical simulations, it is crucial to verify the findings through an experimental investigation. For this reason, an exclusive experimental facility was developed and built internally to evaluate the thermal performance of transformer radiators. The aforementioned facility possesses the capability of assessing the cooling effectiveness of radiators in both AN and AF cooling modes, as illustrated in Figure 7. It is imperative to emphasize that tests were exclusively conducted for the AN-cooling setup. The experimental setup consisted of six radiators that were securely attached to headers. The activation or deactivation of each radiator can be achieved by manipulating the valve positioned at both its inlet and outlet. The monitoring of the inlet oil temperatures and oil flow rates for each radiator was conducted using an IFM SA5000[®] (IFM Electronic GmbH SA5000, Essen, Germany) oil flow sensor, while the monitoring of the oil outlet temperatures was carried out using a Qualitrol[®] PT100 (Qualitrol, Fairport, New York, NY, USA). In addition, a single IFM SA5000[®] (IFM Electronic GmbH, Essen, Germany) oil flow sensor was employed to control the aggregate oil flow within the pipeline responsible for collecting the outlet of the radiators. The data acquisition system employed for the monitoring of flow and temperature sensors was the Elimko E-680[®] (Elimko, Ankara, Türkiye). To maintain thermal equilibrium and counteract the expansion of the oil, a conservator was positioned above the header.

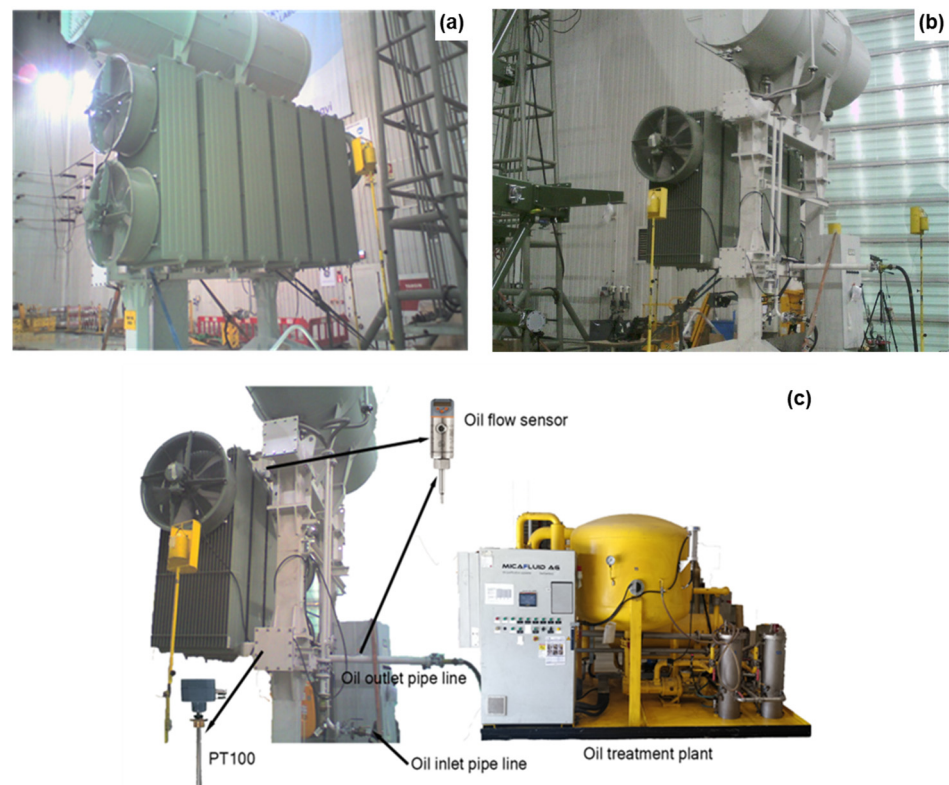


Figure 7. Experiment facility (a) front view, (b) back view, and (c) schematic illustration of the system.

The mineral oil utilized in experiments and simulations exhibits a decomposition temperature of $140\text{ }^{\circ}\text{C}$. Directly heating the transformer oil with a resistor is deemed inappropriate due to the elevated temperature of the resistor surface, which can reach $350\text{ }^{\circ}\text{C}$, leading to the degradation of the transformer oil. The accuracy of numerical computations will be compromised by the modified viscosity and other altered properties of the degraded oil. The utilization of a particular methodology and the meticulous consideration of this issue are of utmost importance when applying heat to the oil. To mitigate the presence of uncertainties, an experimental setup incorporating a MicaFluid VOP200R[®] (MicaFluid, Schlieren, Switzerland) oil treatment plant, equipped with temperature and oil flow control mechanisms, was employed. This setup facilitated the heating of the oil and ensured a consistent cyclic process. The observed phenomenon can be attributed to the simulated internal heating resulting from the core and windings within the transformer. The heated oil was introduced into the conservator, subsequently distributed to the radiators, and underwent cooling as it passed through the radiators, ultimately returning to the MicaFluid VOP200R[®] (MicaFluid, Schlieren, Switzerland) oil tank. The circulation loop was sustained until a state of equilibrium was achieved. Following the attainment of a stable condition, the FLIR T865 (FLIR, Wilsonville, US) thermal imaging camera was employed to visually represent the temperature distribution across the radiators and other components, as depicted in Figure 8.

The experiments were carried out within a controlled laboratory environment that was completely enclosed to minimize any potential interference from air currents that could potentially impact the accuracy of the measurements. The ambient temperature was assessed by employing four measuring points carefully placed around the experimental setup and subsequently calculating the average of these recorded temperatures. The experimental study employed radiators with dimensions of 2300 mm in length, 520 mm in width, and 23 fins. The radiators were positioned with a spacing of 500 mm between their axes. The temperatures of the oil were measured at both the inlet and outlet points of each radiator. Upon an examination of the oil inlet and outlet temperatures, it was observed that the recorded values exhibited a minimal deviation of $\pm 0.2\text{ }^{\circ}\text{C}$ between radiators. In

order to minimize computational expenses and time, a solitary radiator was employed during the validation simulations. The inlet temperature values of radiator number 3 were utilized for comparison with the simulation outcomes. It is important to acknowledge that the comprehensive uncertainty associated with the determination of the cooling capacity was quantified at 5.6%.



Figure 8. Temperature distribution over the radiators and other parts.

The total cooling capacity was compared between the experimental and numerical results, with consideration for different oil flow rates. In this section, we provide an account of the validation process for the numerical model by conducting a comparative analysis between the computed outcomes and the experimental data. A satisfactory level of agreement was observed between the results obtained from numerical simulations and experimental measurements with respect to the overall cooling capacity. Under conditions of steady-state, the observed cooling capacity of a single radiator was recorded as $Q_{T\text{-exp}} = 8335 \text{ W}$ for an oil mass flow rate of 0.25 kg/s . This value was approximately 3.5% lower than the computed cooling capacity obtained from the simulation, which was $Q_{T\text{-CFD}} = 8678 \text{ W}$. The extent of this deviation increased as the mass flow rate increased. The experimentally determined value for $Q_{T\text{-exp}}$ was $23,693 \text{ W}$, whereas the simulation results yielded a value of $Q_{T\text{-CFD}} = 27,495 \text{ W}$ for a flow rate of 1.5 kg/s , resulting in a deviation of 16%. The mean Q_T variation observed between the simulated data and the experimental results was approximately 9.8%, as depicted in Figure 9. It is important to acknowledge that parametric simulations were performed at a flow rate of 0.25 kg/s , resulting in a discrepancy of 3.5% between the simulated values and the measured data. The acceptability of this discrepancy is attributed to the inherent uncertainties associated with temperature and oil flow rate measurements, which can be related to the limitations of the measuring instruments' accuracy. A contributing factor to this discrepancy is the omission of the influence of neighboring radiators in the radiator simulation, which was a significant factor in the experimental measurements. Additionally, the deviation can be attributed to the heat losses incurred by the oil piping system in the experimental setup. In the field of engineering, a certain degree of tolerance for inaccuracy is acceptable, considering the specific objectives of the ongoing investigation. The results indicate that the 3D CFD-based modeling, as proposed, was effectively executed and experimentally validated. The demonstrated efficiency and accuracy of the proposed method further support its efficacy.

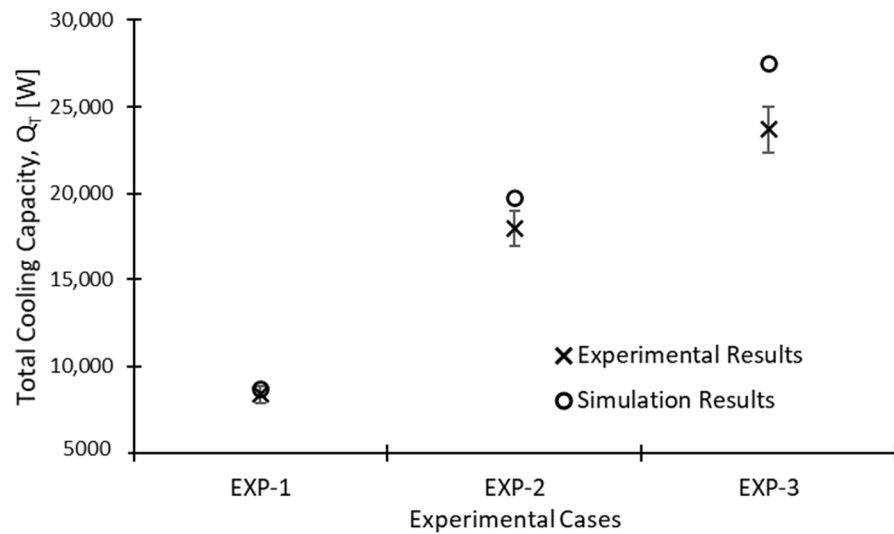


Figure 9. Validation results.

4. Results and Discussion

This section provides the numerical findings pertaining to various configurations of ONAN radiator cooling. The numerical findings are presented in three distinct sections. As previously stated, the main aims of this simulation study are to assess the thermal performance of the radiator under different configurations and dimensions and to optimize the dimensions and configurations based on techno-economic considerations for varying cooling loads. Within the given context, the optimization criteria were determined to be the height of the radiator (L), the spacing between fins (D), and the number of fins (N) present in a radiator. The assessment of these three parameters is imperative due to their interdependent nature. Within this particular context, the simulations were classified into two discrete sections: one aimed at ascertaining the gap size of each radiator fin, and the other focused on examining the height and quantity of the radiator fins. A comprehensive analysis was conducted on an array of 76 sets of radiators. The results obtained were subsequently utilized to conduct an optimization analysis. Prior to conducting techno-economic investigations, the determination of general design limits was defined in the following manner:

- Radiator length (L): 1000–3000 mm
- Number of radiator fins (N): 11–35
- Distance between radiator fins (D): 35–50 mm

It is important to note that the ranges of these parameters were set based on the information provided by the manufacturer. The process of conducting simulations involves two distinct phases. A total of 27 analyses were conducted during the initial phase to investigate the impact of the spacing between the radiator fins on the cooling efficiency, as documented in Table 2. Following the determination of the optimal distance, the combined impact of the remaining two parameters was investigated.

Table 2. Design parameter values for the 1st phase of simulations.

Design Parameter	Radiator Length (L) [mm]	Number of Radiator Fins (N)	Distance Between Fins (D) [mm]	Total Number of Configurations
Minimum Value	1000	11	35	27
Maximum Value	3000	35	50	
Number of Parameters	3	3	3	

4.1. Temperature and Velocity Patterns

The objective of this study is to propose an enhanced cooling arrangement for transformers, with the intention of minimizing the expenses associated with the radiators. To achieve this, a broad analysis of the temperature distribution, flow patterns, and heat transfer mechanisms within a transformer is performed. Nevertheless, in order to obtain a global opinion of the temperature and air velocity distributions within the simulated area, an analysis of the temperature and velocity patterns was conducted once the radiator cooling capacity had reached a steady-state regime. It is important to acknowledge that the 17th radiator configuration in Table 3 is regarded as a representative model for post-processing.

Table 3. Effect of distance between fins on the thermal performance of the radiator.

Configuration Number	Design Parameter			Performance Parameter	
	L [mm]	N	D [mm]	T _{oil,out} [°C]	Q _T [W]
1	1000	11	35	48.80	3021
2	1000	11	42.5	48.78	3033
3	1000	11	50	48.74	3054
4	1000	23	35	42.77	5963
5	1000	23	42.5	42.72	5989
6	1000	23	50	42.61	6042
7	1000	35	35	37.22	8668
8	1000	35	42.5	37.14	8707
9	1000	35	50	36.94	8806
10	2000	11	35	46.56	4113
11	2000	11	42.5	46.52	4136
12	2000	11	50	46.39	4195
13	2000	23	35	38.96	7821
14	2000	23	42.5	38.87	7862
15	2000	23	50	38.63	7982
16	2000	35	35	32.70	10,872
17	2000	35	42.5	32.53	10,954
18	2000	35	50	32.17	11,127
19	3000	11	35	43.47	5620
20	3000	11	42.5	43.37	5672
21	3000	11	50	43.18	5764
22	3000	23	35	35.64	9438
23	3000	23	42.5	35.31	9600
24	3000	23	50	34.89	9805
25	3000	35	35	29.19	12,585
26	3000	35	42.5	28.75	12,796
27	3000	35	50	28.16	13,083

Figures 10 and 11 illustrate the ONAN-cooling model, depicting the flow and temperature fields of the cooling air surrounding the radiators. These observations reveal the characteristic features of natural convection, which is driven by the buoyancy force resulting from the temperature disparity between the ambient cooling air and the heated oil. Due to natural convection, the surrounding cool air adjacent to the radiators is drawn into the spaces between the fins affixed to the radiators, subsequently ascending along these fin gaps. The process of natural convection causes the ambient cooling air to ascend along the outer surface of the radiators. The upward movement of cooling air through the gaps between the radiator fins and along the outer surface of the radiators leads to an increase in its velocity. This acceleration in flow is caused by the buoyancy force. Additionally, the temperature of the cooling air rises due to heat transfer from the hot oil to the cooling air through the radiators.

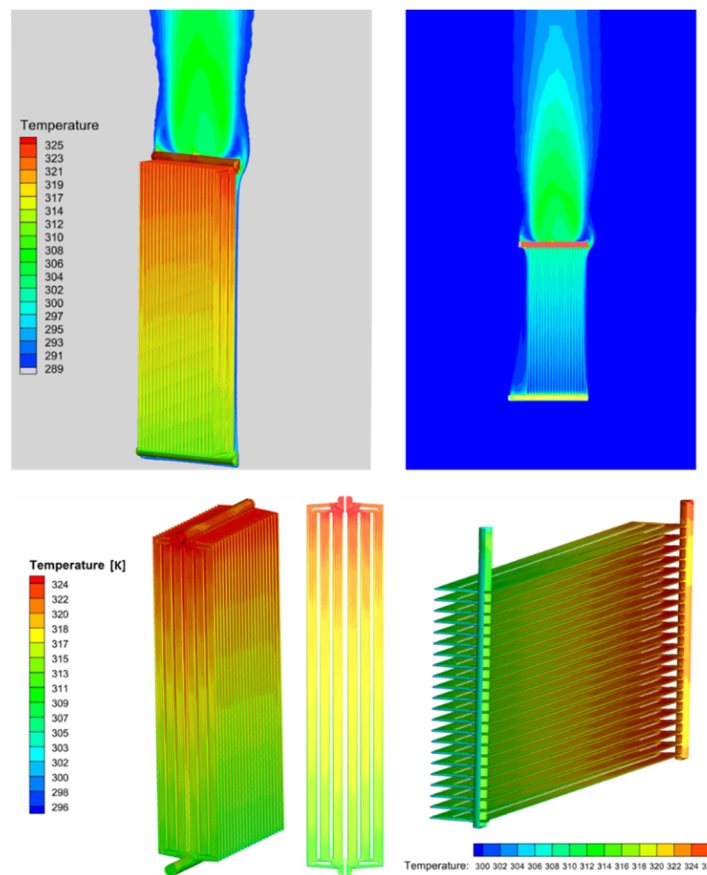


Figure 10. The temperature profile.

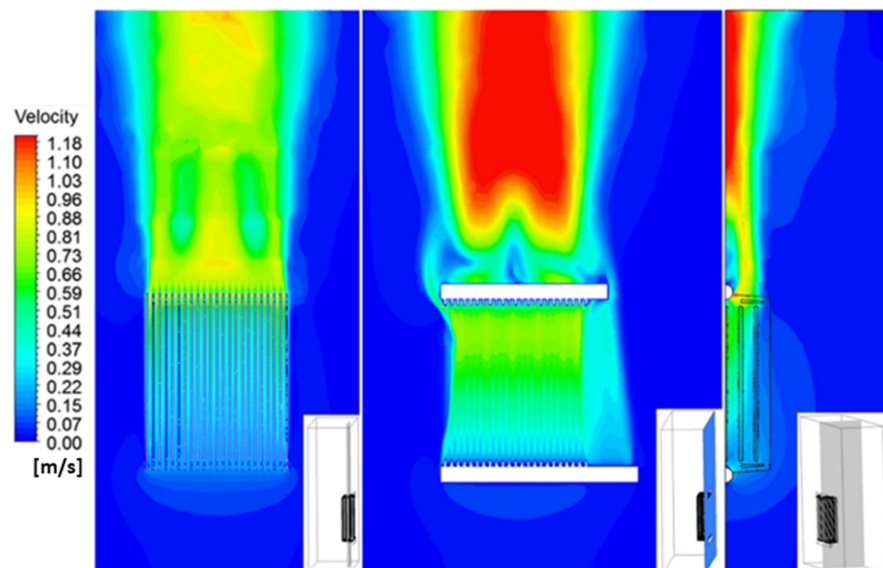


Figure 11. The air velocity profile.

The data presented in Figure 10 indicate that the average surface temperature of the fins located at the edge is comparatively lower than that of the fins situated in the middle. The mean surface temperature at the outer edges of the fin is approximately 44.1 °C, whereas the corresponding value at the center is 46.5 °C. This discrepancy arises from the fact that the outer fins are in direct contact with the surrounding still air, while the inner fins are subjected to airflow that has been heated to a higher temperature as a result of heat exchange between the hot oil and the cooling air passing through the attached

radiators. Furthermore, the view factor for the inner fins is significantly reduced due to their limited ability to emit heat solely through the gaps located between the radiator fins on the sides, top, and bottom. Conversely, when examining the behavior of air temperature, it is observed that at lower elevations, it closely approximates the reference value of 19 °C. However, in the middle section, it fluctuates between 22 °C and 28 °C. In the uppermost range, the temperature exhibits variability between 27 °C and 32 °C, with a mean value of 29 °C. It is noteworthy to mention that the average heat transfer coefficient of air for the simulated model was determined to be 9.7 W/m²·K through the utilization of the following expressions:

$$\bar{h} = \frac{Q_T}{A_s(T_{oil,avg} - T_{a,\infty})} \tag{5}$$

$$T_{oil,avg} = \frac{T_{oil,in} - T_{oil,out}}{2} \tag{6}$$

Figure 11 displays the velocity contours observed at various planes across the width and height of the radiator. The air velocity at the lower position exhibits fluctuations ranging from 0.14 m/s to 0.23 m/s, with an average value of 0.18 m/s. Following an increase in temperature, the air likewise exhibits an increase in velocity. In the intermediate height range (1200 mm), the velocity exhibits a range of 0.1 m/s to 0.7 m/s, with an average value of 0.6 m/s. In the uppermost section, the velocity varies between 0.4 m/s and 0.9 m/s, with an average value of 0.75 m/s. The air velocity between two panels exhibits a strong correlation with the air flow that enters the radiator via its lateral sides. The lateral flow additionally alters the ambient air temperature and the coefficient of heat transfer.

4.2. Effect of the Fin Distance

This section examines the impact of the spacing between the fins on the cooling efficiency of the radiator. The design parameters and performance values of the geometries are provided in Table 3.

Upon examination of the obtained results, as presented in Table 3, it can be observed that for an L of 3000 mm, N = 35, and D = 35 mm (Config. 25), the value of Q_T is determined to be 12,585 W. Similarly, for D = 42.5 mm (Config. 26), the value of Q_T is found to be 12,796 W. Finally, for D = 50 mm (Config. 27), the value of Q_T is determined to be 13,083 W. When the D is increased from 35 mm to 42.5 mm, there is an accompanying increase in Q_T of 1.7%. Similarly, when the D is increased from 35 mm to 50 mm, the Q_T increases by 4%. This phenomenon is observed in various configurations, albeit with a diminishing impact of distance on smaller radiators in relation to their height and weight. As an illustration, when the L is set to 1000 mm and the N is 11, the cooling capacity exhibits a 0.41% increase as the D is extended from 35 mm (Config. 1) to 42.5 mm (Config. 2). Similarly, when the D is further increased from 42.5 mm to 50 mm (Config. 3), the Q_T exhibits a 1.1% increase. Upon examination of the mean values across all configurations, it is observed that when the L is 42.5 mm, the Q_T is approximately 0.8% greater than that of L = 35 mm. When the D is extended to 50 mm, there is an observed change in the value of Q_T, amounting to approximately 2.3%. The findings indicate that a 50 mm gap between the fins yields the most optimal cooling performance. However, it is observed that variations in the gaps between the radiator fins have a minimal influence on the overall cooling capacity. Therefore, in the subsequent stage of the parametric analysis, a distance of 50 mm is selected, which represents the spacing between the fins.

4.3. Techno-Economic Investigations

In this section, the response surface method (RSM) is employed to optimize the geometry of the radiator. The thermal performance of the examined distribution transformer was simulated in accordance with the methodology outlined in the preceding sections. Subsequently, the Q_T and the associated cost of the cooling system were identified as the essential output parameters for the optimization study. The estimation of the relationship between the independent variables and the response, specifically the Q_T and cost,

was conducted through the utilization of the design of experiments methodology. The utilization of RSM optimization offers greater benefits compared with conventional single parameter testing methodologies, which solely examine the impacts of individual factors on the variable [34]. Furthermore, the RSM can be utilized to construct empirical models that establish correlations between the response variable and the influential factors.

The techno-economic performance of a transformer can be influenced by various geometrical specifications, as determined by the configuration of its cooling system. Hence, the primary variables encompass the dimensions of the oil channel, fin width, fin height, fin length, fin vertical position, fin spacing, and the quantity of the fins. Taking into account all seven parameters, the RSM will generate numerous cases wherein the ANSYS-Fluent[®] software will be utilized to ascertain the value of the total cooling capacity. The time-consuming and computationally expensive nature of considering all parameters in RSM is attributed to the intricate nature of the problem. Hence, the identification of the most crucial parameters was conducted in order to minimize the quantity of parameters needed. Among the parameters considered, three were identified as having a significant impact on the techno-economic performance of the transformer radiator. These parameters are the fin height (L), number of fins (N), and spacing between fins (D). The aforementioned parameters were identified as the most influential factors affecting the thermal performance of radiators in the existing literature [23]. The spacing parameter was analyzed separately, whereas the remaining two input parameters were studied jointly. Figure 12 illustrates the procedure employed for conducting a techno-economic investigation.

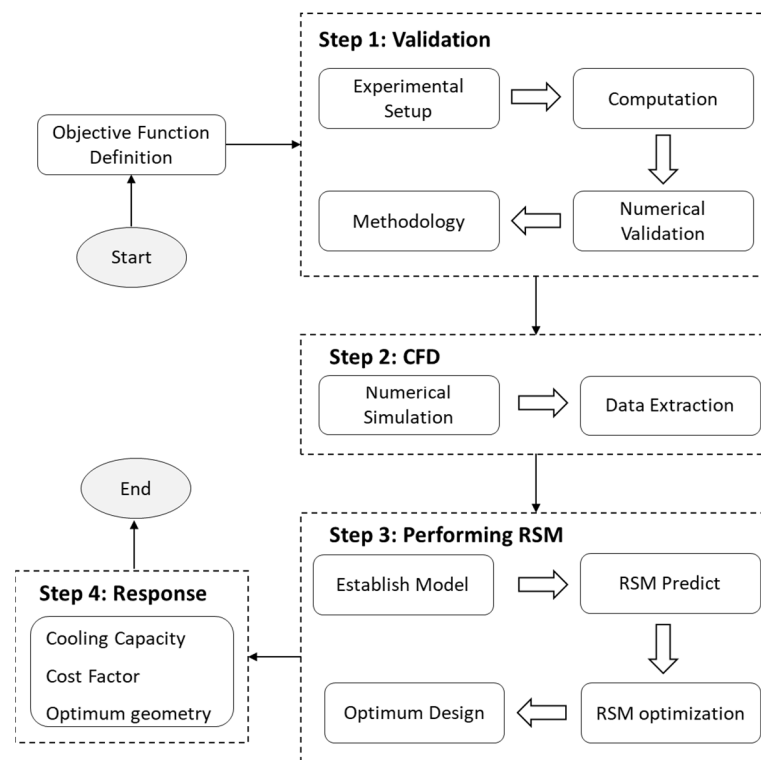


Figure 12. Flow chart.

It is important to acknowledge that the RSM analysis assigned equal weight to the input parameters of cost and cooling capacity. To facilitate the development of a RSM model for optimization purposes, a comprehensive set of 49 CFD analyses were performed under specific conditions. After conducting all the necessary analyses to establish the RSM model, it becomes obvious that there is a statistically significant correlation between the response parameters and the input parameters. The error metric (R^2) for the Q_T was found to be 0.99.

Based on the aforementioned discussion, the geometries of the actual transformer cooling systems were taken into account when determining the two main design parameters, L and N, which were treated as independent variables. A variety of combinations of the variables were identified within a specified range, ranging from L = 2000 mm and N = 18 to L = 3000 mm and N = 30. The Q_T and the overall cost linked to each case were ascertained through the execution of a numerical simulation. To determine the overall cost, the initial step involved the calculation of the dimensions of the radiator walls and the corresponding oil volumes. These values were then multiplied by the appropriate density to obtain the individual masses of steel and oil. This was undertaken to facilitate the subsequent economic analysis. The average cost or range of the tanks and radiators (%) in the total material cost of a power transformer are given in Table 4. The unit costs for steel and radiator oil are 3.3 EUR/kg and 1.5 EUR/kg, respectively. The Q_T values that were determined were divided by the cost associated with each radiator configuration.

Table 4. Ratio of the average cost of tank and radiators to the total material cost of a power transformer.

Types	Rating [MVA]	Tank Cost [%]	Radiator Cost [%]
Large-range power transformers	54.6	8.45	0.23338
Medium-range power transformers	54.6	12.85	0.23299
Small-range power transformers	54.6	17.80	0.23152

Subsequently, the resulting capacity values per unit cost were calculated in terms of W/EUR. The simulations consider an experimentally derived mass flow rate of 0.250 kg/s and an oil inlet temperature of 55 °C for the internal flow of oil. In the case of external air flow, the ambient temperature was assumed to be 15 °C. The specific heat value and density of oil were determined by considering average oil temperatures and were derived through the process of interpolating the thermophysical properties provided for mineral oil. Table 5 presents a comprehensive overview of the various runs conducted, covering important details such as the total cooling capacity and associated costs.

Table 5. Design parameters and techno-economic analysis results of different radiators.

No.	Radiator Length [mm]	Number of Fin	Steel Volume [m ³]	Steel Mass [kg]	Steel Cost [€]	Oil Volume [m ³]	Oil Density [kg/m ³]	Oil Mass [kg]	Oil Cost [€]	Total Cost [€]	Cooling Capacity Q_T [W]	Q_T /Cost [W/€]
1	2000	18	0.0412	322.3	1063.5	0.0962	859.8	82.7	124.1	1188	6796	5.72
2	2000	20	0.0456	357.4	1179.5	0.1067	860.1	91.8	137.7	1317	7560	5.74
3	2000	22	0.0501	392.6	1295.6	0.1172	860.4	100.8	151.3	1447	7782	5.38
4	2000	24	0.0546	427.8	1411.7	0.1277	860.9	109.9	164.9	1577	8284	5.25
5	2000	26	0.0591	463	1527.8	0.1382	861.2	119	178.5	1706	8693	5.09
6	2000	28	0.0636	498.1	1643.8	0.1487	861.5	128.1	192.1	1836	9089	4.95
7	2000	30	0.0681	533.3	1759.9	0.1592	861.7	137.2	205.7	1966	9325	4.74
8	2200	18	0.0457	358.1	1181.6	0.1046	860	90	135	1317	7211	5.48
9	2200	20	0.0507	397.2	1310.8	0.1161	860.4	99.9	149.8	1461	7750	5.31
10	2200	22	0.0557	436.4	1440	0.1275	860.8	109.7	164.6	1605	8169	5.09
11	2200	24	0.0607	475.5	1569.2	0.1389	861.1	119.6	179.4	1749	8595	4.92
12	2200	26	0.0657	514.7	1698.4	0.1504	861.5	129.5	194.3	1893	9025	4.77
13	2200	28	0.0707	553.8	1827.6	0.1618	861.8	139.4	209.1	2037	9417	4.62
14	2200	30	0.0757	593	1956.8	0.1732	862.1	149.3	224	2181	9795	4.49
15	2400	18	0.0503	393.9	1299.7	0.1131	860.3	97.3	145.9	1446	7635	5.28
16	2400	20	0.0558	437	1442.1	0.1254	860.7	108	161.9	1604	8168	5.09
17	2400	22	0.0613	480.1	1584.4	0.1378	861.1	118.7	178	1762	8545	4.85
18	2400	24	0.0668	523.2	1726.7	0.1502	861.4	129.4	194	1921	9004	4.69
19	2400	26	0.0723	566.4	1869	0.1625	861.8	140.1	210.1	2079	9438	4.54
20	2400	28	0.0778	609.5	2011.4	0.1749	862.1	150.8	226.2	2238	9837	4.40
21	2400	30	0.0834	652.6	2153.7	0.1873	862.4	161.5	242.3	2396	10,217	4.26
22	2500	18	0.0526	411.8	1358.8	0.1173	860.5	100.9	151.4	1510	7816	5.18
23	2500	20	0.0583	456.9	1507.7	0.1301	860.9	112	168	1676	8319	4.96
24	2500	22	0.0641	502	1656.6	0.1429	861.2	123.1	184.7	1841	8706	4.73
25	2500	24	0.0699	547.1	1805.5	0.1558	861.6	134.2	201.3	2007	9207	4.59
26	2500	26	0.0756	592.2	1954.4	0.1686	862	145.3	218	2172	9640	4.44
27	2500	28	0.0814	637.4	2103.3	0.1815	862.3	156.5	234.7	2338	10,039	4.29
28	2500	30	0.0872	682.5	2252.1	0.1943	862.6	167.6	251.4	2504	10,396	4.15
29	2600	18	0.0549	429.7	1417.9	0.1215	860.6	104.5	156.8	1575	7939	5.04
30	2600	20	0.0609	476.8	1573.3	0.1348	861	116.1	174.1	1747	8417	4.82
31	2600	22	0.0669	523.9	1728.8	0.1481	861.4	127.6	191.3	1920	8909	4.64
32	2600	24	0.0729	571	1884.2	0.1614	861.8	139.1	208.6	2093	9381	4.48
33	2600	26	0.0789	618.1	2039.7	0.1747	862.1	150.6	225.9	2266	9813	4.33

Table 5. Cont.

No.	Radiator Length [mm]	Number of Fin	Steel Volume [m ³]	Steel Mass [kg]	Steel Cost [€]	Oil Volume [m ³]	Oil Density [kg/m ³]	Oil Mass [kg]	Oil Cost [€]	Total Cost [€]	Cooling Capacity Q _T [W]	Q _T /Cost [W/€]
34	2600	28	0.085	665.2	2195.1	0.188	862.4	162.1	243.2	2438	10,211	4.19
35	2600	30	0.091	712.3	2350.6	0.2013	862.8	173.7	260.5	2611	10,594	4.06
36	2800	18	0.0594	465.5	1536	0.1299	860.9	111.8	167.8	1704	8309	4.88
37	2800	20	0.066	516.5	1704.6	0.1442	861.3	124.2	186.2	1891	8782	4.64
38	2800	22	0.0725	567.6	1873.2	0.1584	861.7	136.5	204.7	2078	9283	4.47
39	2800	24	0.079	618.7	2041.7	0.1726	862.1	148.8	223.2	2265	9748	4.30
40	2800	26	0.0855	669.8	2210.3	0.1869	862.4	161.2	241.7	2452	10,171	4.15
41	2800	28	0.0921	720.9	2378.9	0.2011	862.8	173.5	260.3	2639	10,582	4.01
42	2800	30	0.0986	772	2547.5	0.2154	863.1	185.9	278.8	2826	10,951	3.87
43	3000	18	0.064	501.3	1654.1	0.1383	861.1	119.1	178.7	1833	8586	4.68
44	3000	20	0.071	556.3	1835.8	0.1535	861.5	132.3	198.4	2034	9103	4.47
45	3000	22	0.0781	611.4	2017.6	0.1687	861.9	145.4	218.1	2236	9607	4.30
46	3000	24	0.0851	666.4	2199.3	0.1839	862.3	158.6	237.8	2437	10,056	4.13
47	3000	26	0.0921	721.5	2381	0.199	862.7	171.7	257.6	2639	10,522	3.99
48	3000	28	0.0992	776.6	2562.7	0.2142	863.1	184.9	277.3	2840	10,931	3.85
49	3000	30	0.1062	831.6	2744.4	0.2294	863.4	198.1	297.1	3041	11,294	3.71

The further assessment in this research is devoted to a detailed analysis of the sensitivity of input factors affecting heat transfer in the context of radiator design and optimization. There is a strong correlation between geometric parameters and heat transfer, as shown in Figure 13. Upon analyzing the outcomes of the fixed L and varying N, it is observed that the thermal capacity exhibits a linear growth pattern in accordance with the increase in N, as anticipated. Similarly, when the L increases for a given value of N, there is an increase in heat transfer.

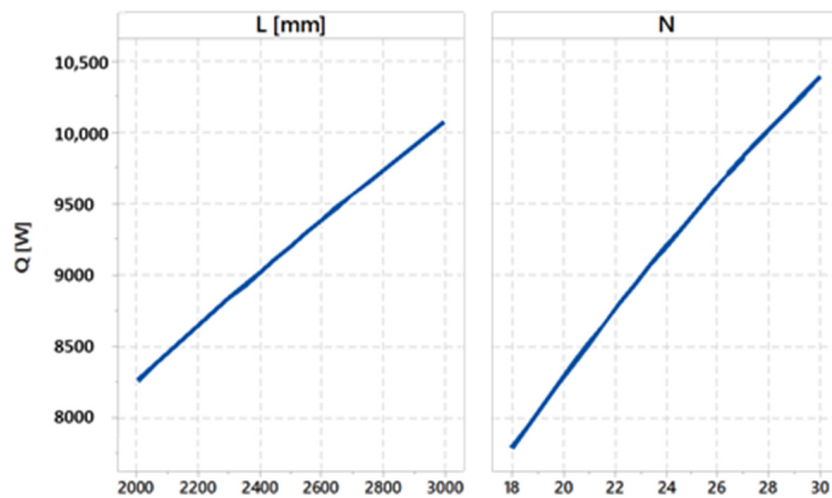


Figure 13. Relationship between geometric parameters and heat transfer.

Furthermore, Figure 14 depicts the surface plot representing the heat transfer as a function of the variables L and N. The heat transfer response can be determined by employing the following equation, wherein Q_T denotes the cooling capacity.

$$Q_T = -2219 + 2.10L + 326N - 1.52 \times 10^{-4}L^2 - 3.27N^2 + 0.0193L \times N \quad (7)$$

The cost equation is also derived using the RSM. As predicted, a strong correlation was observed between the cost factor and geometric details, as shown by the following equation.

$$\text{Cost} = 22.73 \times 1.09 \times 10^{-3}L - 6.97N + 10^{-7}L^2 + 1.2 \times 10^{-3}N^2 + 0.0358L \times N \quad (8)$$

Based on the findings presented in Table 5, it is evident that the radiator configuration with the highest cooling capacity per unit investment cost (Q_T/Cost) is observed in the largest radiator configuration (No. 49). A decrease in the size of the radiator results in an increase in the cooling capacity per unit cost. Hence, it is not possible to assert that the largest radiator configuration is the most techno-economically optimal based on the available data. Nevertheless, a crucial inquiry emerges concerning which combination provides the most cost-effective factor for the desired heat transfer parameter. Given these objectives, the cost factor is also examined. The results obtained from this comprehensive investigation provide significant contributions to the body of knowledge in the area of heat transfer optimization. Through the acknowledgement of the significant relationship between geometric parameters and heat transfer and the consideration of cost implications, individuals involved in research, engineering, and practical applications can make accurate decisions when designing or optimizing systems to achieve improved thermal performance and cost-effectiveness. Hence, it is imperative to determine the optimal N and L values that yield the lowest cost for the desired cooling capacity. In order to determine the optimal values of L and N that minimize the investment cost for desired cooling capacities (Q_T), an optimizer in the Minitab v19[®] program was utilized. The findings of this analysis are presented in Table 6 and Figure 15.

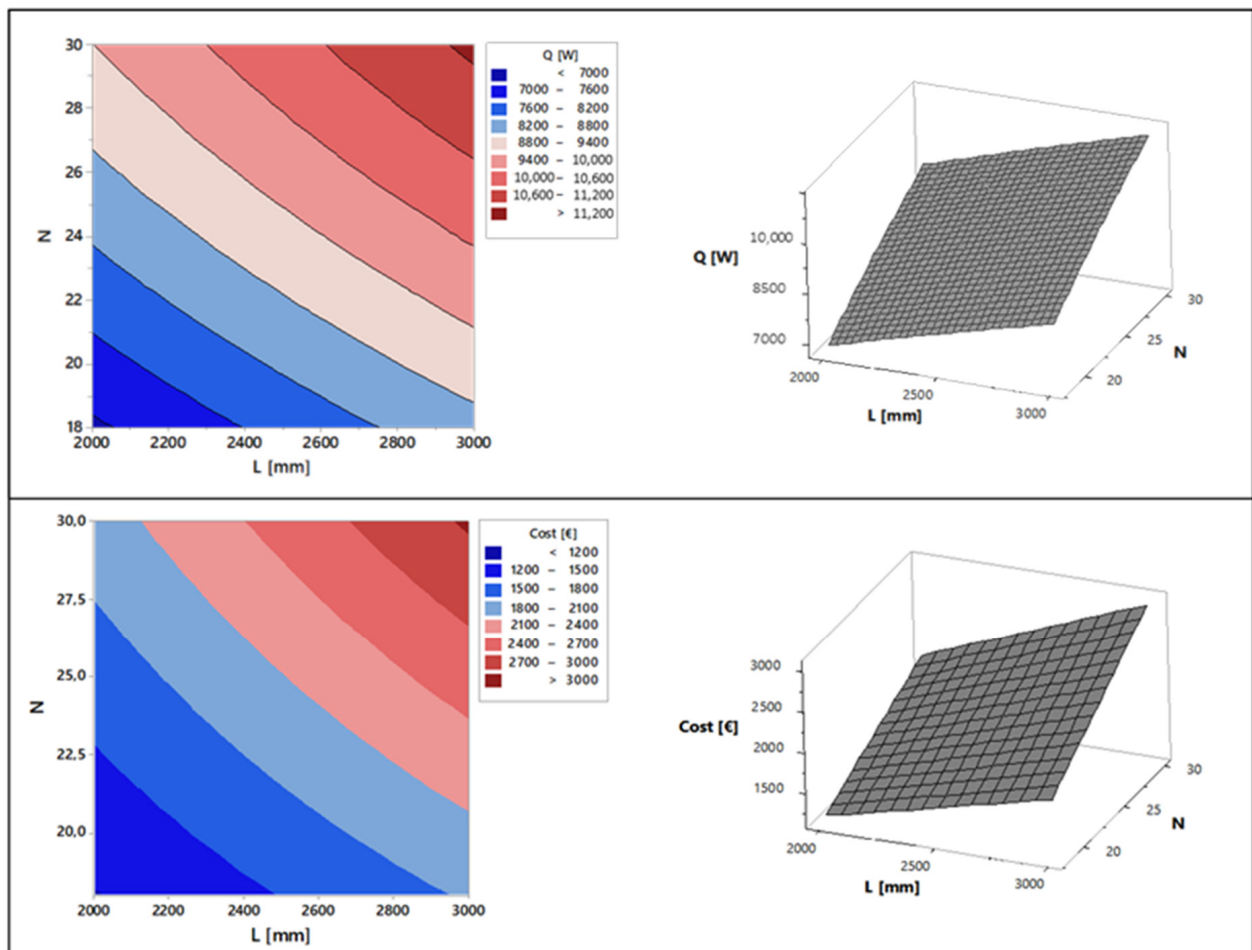


Figure 14. Effect of radiator length and number of fins on cooling capacity and cost.

Table 6. Optimization results.

Cases	Optimum Combination		Cost Fit [€]	Q _T Fit [W]
	L [mm]	N		
1	2000	18	1187.5	6895
2	2015	18	1217.8	7000
3	2049	19	1291.3	7250
4	2078	20	1366.8	7500
5	2102	21	1444.2	7750
6	2122	22	1523.6	8000
7	2136	23	1604.9	8250
8	2145	24	1688.0	8500
9	2148	25	1773.0	8750
10	2144	26	1859.8	9000
11	2131	28	1948.3	9250
12	2108	29	2038.4	9500
13	2325	28	2186.2	9750
14	2371	29	2304.4	10,000
15	2428	30	2426.6	10,250
16	2557	30	2565.8	10,500
17	2690	30	2708.0	10,750
18	2825	30	2853.3	11,000
19	2963	30	3002.0	11,250
20	3000	30	3008.9	11,261

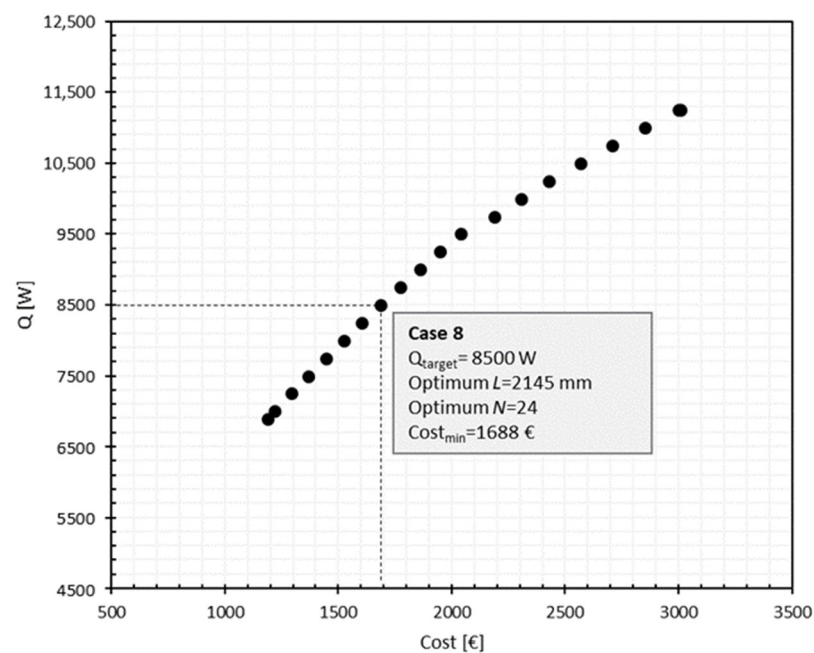


Figure 15. The relationship between cooling capacity and the cost factor.

The correlation between the cooling capacity and the cost factor for Case 8, as illustrated in Table 6, is visually represented in Figure 15. This graphical representation offers additional understanding of the system’s performance and economic implications. Upon analyzing the obtained results, it becomes apparent that, when considering a specific case as a study, the attainment of a cooling capacity of 8500 W requires a length of $L = 2145$ mm, with $N = 24$ individual fins, under the optimized condition that minimizes cost. Nevertheless, by referring to the dimensions provided in Table 6, one can select the most suitable radiator geometry, characterized by $L = 2200$ mm, $N = 24$, and $D = 50$ mm.

Figure 16, which presents a graphical representation of the findings outlined in Table 6, visually depicts the influence of variables L and N on the cooling capacity while consider-

ing a condition of minimum cost. The graph illustrates a distinct correlation between the aforementioned variables and the corresponding cooling capabilities they provide. The findings highlight the critical role of L and N in determining the efficacy of the system's cooling process. The favorable impact of these variables on the cooling capacity implies that by optimizing both L and N, substantial improvements in cooling performance can be achieved without compromising cost-effectiveness. By integrating this knowledge into the design process, engineers and researchers will have the ability to customize radiator configurations in order to fulfill specific cooling demands while avoiding unnecessary expenses.

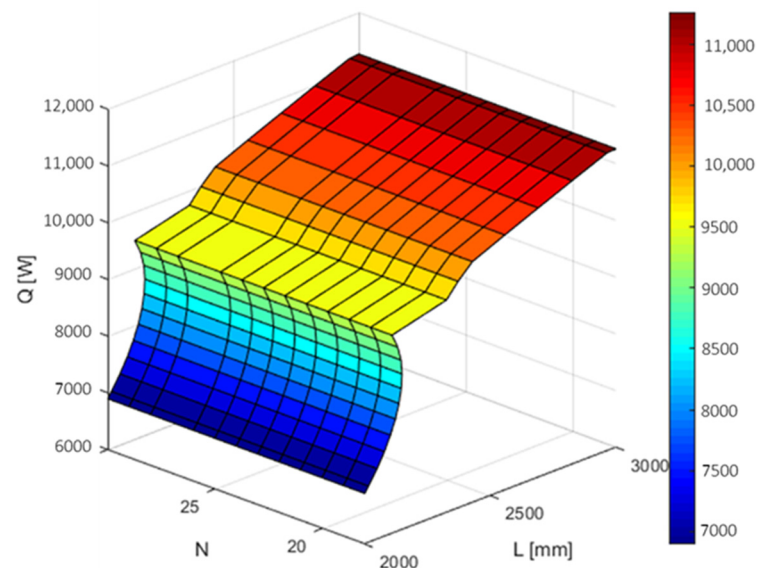


Figure 16. Response surface plot cooling capacity against optimum combination of length and the fin number.

5. Conclusions

The durability and reliability of a power transformer are significantly influenced by the methods employed for cooling, as the primary factor leading to the degradation of insulation performance is the excessive generation of heat. It is imperative to implement an optimal cooling design in order to prevent operational malfunctions and material deterioration resulting from thermal harm. In this research, transformer radiator configurations in ONAN mode yielded designs with the lowest cost for the desired cooling capacities. The aforementioned objective was successfully accomplished by implementing the subsequent procedures. The simulation of the flow and temperature fields within the radiator, as well as the surrounding ambient air and solid components, was conducted using the Ansys Fluent 2023 R1[®] software, which is a widely used commercial CFD tool. This analysis aimed to investigate the distribution of velocity and temperature within the insulating oil (mineral oil) inside the radiator, as well as the cooling air outside the radiator and the temperature distribution within the solid components of the radiator. A total of 76 radiator configurations were investigated. Following this, the acquired findings were employed to carry out an optimization analysis. The simulations were conducted using a high-performance computing system comprising 500 processors. Subsequently, the numerical model was validated using the experimental data. The experimental investigations were conducted at the research facilities of General Electric Grid Solutions. The input data for the techno-economic optimization study consisted of the results obtained from the CFD simulations. Finally, the RSM was employed, utilizing the commercially available statistical software MINITAB v19[®]. The objective was to determine the most efficient radiator configuration that would provide the desired cooling capacity while minimizing costs. The aforementioned study's findings yielded the following conclusions:

The findings of the techno-economic analysis indicate that optimizing both parameters L and N can result in notable improvements in cooling capacity, without compromising cost-effectiveness. Significant correlations were found between the cost factor and geometric detail. The findings indicate that the cooling performance is maximized when the gap between the fins is 50 mm. However, the gaps between the radiator fins have minimal influence on the overall cooling capacity. A decrease in the size of the radiator results in an increase in the cooling capacity per unit cost. The calculated average heat transfer coefficient of air for the simulated model is $9.7 \text{ W/m}^2\cdot\text{K}$. When examining the optimal geometries from a techno-economic perspective, it becomes evident that increasing the number of fins is a more rational approach for enhancing cooling capacity, as opposed to increasing the length of the radiator fins.

The results obtained from this extensive analysis provide significant contributions to the field of heat transfer optimization. Researchers, engineers, and practitioners can make informed decisions in the design or optimization of systems for improved thermal performance and cost efficiency by acknowledging the significant relationship between geometric parameters and heat transfer, while also taking into account cost factors. Regarding future research, it is recommended that further investigations be carried out to analyze the performance of alternative cooling modes within the transformer cooling system.

Author Contributions: Conceptualization, A.K. and O.S.; methodology, A.K., O.S. and H.Ö.; software, A.K. and Ö.A.; validation, O.S. and A.K.; investigation, A.K., O.S., Ö.A. and H.Ö.; writing—review and editing, A.K., O.S., Ö.A. and H.Ö.; project administration, A.K., O.S. and H.Ö.; funding acquisition, A.K. and O.S. All authors have read and agreed to the published version of the manuscript.

Funding: The present study was supported financially by the Scientific and Technological Research Council of Turkey (TUBITAK) through the TEYDEB-3190903 project.

Data Availability Statement: Data are contained within the article.

Acknowledgments: The present study was supported financially by the Scientific and Technological Research Council of Turkey (TUBITAK) through the TEYDEB-3190903 project, with the participation of Koca and Senturk as researchers. The simulation studies were conducted at the facilities of the Turkish Aerospace Industries company. The experimental studies were performed at the facilities of General Electric Grid Solutions company.

Conflicts of Interest: Authors Oguzkan Senturk and Hakan Özcan were employed by the General Electric Grid Solutions company. Author Ömer Akbal was employed by the Turkish Aerospace Industries company. The remaining author declared no conflict of interest.

Nomenclature

A_s	Total surface area of radiator (m^2)
c_p	Total cooling capacity (W)
Cost	Total cooling investment cost (€)
D	Distance between radiator fins (mm)
G	Gravitational acceleration (m/s^2)
\bar{h}	Average heat transfer coefficient ($\text{W/m}^2\cdot\text{K}$)
k_s	Thermal conductivity of fins ($\text{W/m}\cdot\text{K}$)
k_f	Thermal conductivity of fluid ($\text{W/m}\cdot\text{K}$)
L	Fin height (mm)
\dot{m}	Mass flow rate (kg/s)
N	Number of fins
P	Static pressure (Pa)
Q_T	Specific heat at constant pressure ($\text{kJ/kg}\cdot\text{K}$)
T_{air}	Air temperature ($^\circ\text{C}$)
T_{oil}	Oil temperature ($^\circ\text{C}$)
V_a	Air velocity (m/s)

Greek symbols	
B	Coefficient of expansion (1/K)
M	Coefficient of viscosity (Pa.s)
P	Density (kg/m ³)
Abbreviations	
AN	Air-Natural
CFD	Computational Fluid Dynamics
RSM	Response Surface Method
ONAN	Oil-Natural Air-Natural
SST	Shear Stress Transport
S2S	Surface to Surface
Sub/superscripts	
A	Air
Ave	Average
In	Inlet
i,j	Tensor notations
Out	Outlet

Appendix A

The loading capability of a transformer is determined by the absolute temperature, as it directly influences the speed at which insulation materials undergo thermal aging. The cooling system’s design guarantees that the prescribed limits for top oil and winding temperature rise are achieved, effectively regulating the highest temperatures obtained. The temperature rise refers to the variation in temperature between the ambient coolant and specific components of the transformer structure during normal operational loading. Under consistent load and ambient temperature conditions, the temperature of the transformer components will eventually stabilize. The load and ambient temperature vary in accordance with the daily and seasonal changes.

The temperature limitations for a transformer include the Top Oil Rise (TOR), the average or Mean Winding Rise (MWR), and the Hotspot Temperature Rise (HSR). These constraints are predetermined limits that consider the temperature fluctuations that occur over the lifespan of the transformer. The top oil rise calculation is given in the equations below:

$$A_{rad} = A_{pan} \times N_{pan} \times N_{rad} \tag{A1}$$

$$\Delta\theta_{oil} = \Delta\theta_0 \times \left[\frac{P_{tot}}{Q_{tq,0} \times A_{tq} + f \times Q_{rad,0} \times A_{rad}} \right]^n + C_{oil} \tag{A2}$$

where the constants and variables are given in Table A1.

Table A1. Constants and variables—1.

Constants and Variables	Unit	Definition
$Q_{rad,0}$	W/m ²	Exchanged heat per m ² of radiators at $\Delta\theta_0$
$Q_{tq,0}$	W/m ²	Exchanged heat per m ² of tank at $\Delta\theta_0$
$\Delta\theta_0$	K	Reference oil rise
C_{oil}	K	Temperature correction factor
N	-	Constant depending on the ONAN cooling mode
A_{pan}	m ²	Surface area of one radiator panel
A_{rad}	m ²	Total surface area of all radiators
A_{tq}	m ²	Approximate cooling surface of tank
f	-	Effectiveness factor depending on radiator’s topology or on relative air flow
N_{pan}	-	Number of panels per radiator
N_{rad}	-	Number of radiators
P_{tot}	W	Total loss to dissipate
$\Delta\theta_{oil}$	K	Average oil temperature rise above ambient

- Being able to depict the temperature correlations within a transformer is useful. To depict the heating and cooling effects of the transformer, a thermal diagram can be generated by employing specific simplifying assumptions. The necessary assumptions are as follows:
- The ambient temperature is regarded as constant. This ambient temperature serves as the basis for calculating all subsequent temperature increases.
- The oil that flows into the lower part of each coil has the same temperature.
- The oil temperature at the exit of each winding is equivalent to the Top Oil temperature (TO) in the tank.
- It is presumed that the temperature of the oil will rise uniformly across the windings. Despite the larger local eddy losses in the top- and bottom-end areas of the winding, this approximation remains reasonably accurate.
- The mean oil rise (MOR) is calculated as the average of the temperature increases in both the top and bottom layers of oil.
- MWR is calculated by analyzing the electrical resistance measurements of each individual winding in a transformer.
- The difference between the conductor temperature at the mean winding height and the mean cooler oil temperature at the same position, known as the “Winding Gradient” (GR), can be obtained by subtracting the MOR from the MWR.
- Figure A1 displays a typical thermal diagram of a transformer, which refers to the standard IEC temperature rises.

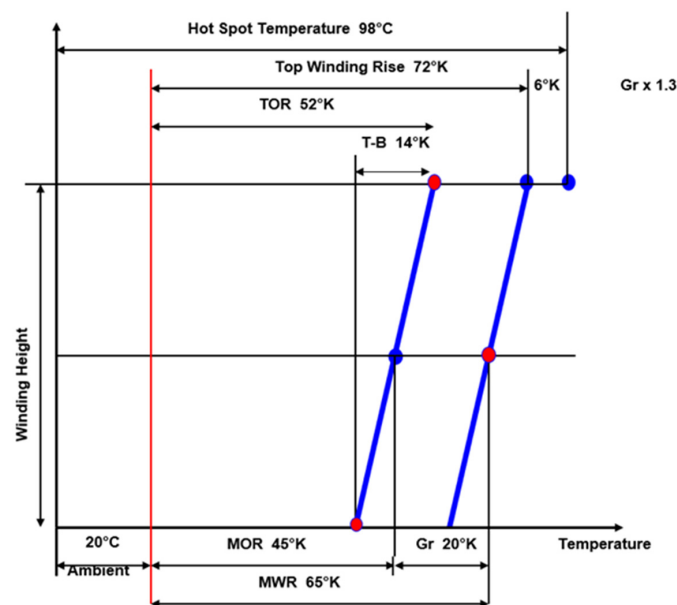


Figure A1. Thermal model of a transformer.

The assumption is made that the gradient of the windings remains constant throughout the entire height of the windings. The average conductor temperature linear graph is thus plotted in line with the oil temperature linear graph. Nevertheless, buried conductors exhibit elevated temperatures compared with the normal winding conductor, and furthermore, there are increased eddy losses in close proximity to the ends of the windings. Consequently, the increase in temperature at the HSR is greater than the sum of the GR and the rise in top oil temperature.

To generate an estimate of the hotspot gradient, one can multiply the winding gradient by a factor that is determined by the additional local loss and temperature. It is feasible to determine a multiplication factor for each winding by considering the local eddy losses. However, in cases where precise data are not accessible, international standards offer approximate values that can be utilized. For power transformers, the IEC now recommends a hotspot multiplying factor of 1.3.

The top oil rise calculation is given in Equation (A5), which is also used for sizing the radiators of a transformer.

$$Q_{rad} = \left(P_{tot} - \left(\frac{\Delta\theta_{oil}}{\Delta\theta_0} \right)^{\frac{1}{n}} \times Q_{tq,0} \times A_{tq} \right) \times \frac{1}{A_{rad}} \tag{A3}$$

$$\Delta\theta_{co} = K_0 \times f_L \times \sqrt{\frac{Q_{rad}}{\Delta h}} \tag{A4}$$

$$\Delta\theta_{topoil} = \Delta\theta_{oil} + \Delta\theta_{co} + C_{topoil} \tag{A5}$$

Table A2. Constants and variables—2.

Constants and Variables	Unit	Definition
C_{topoil}	K	Temperature correction factor
K_0	$m^{1.5}/kW^{0.5}$	ON factor for top oil calculation
Q_{rad}	W/m^2	Calculated total exchanged heat per m^2 of radiators in ON
f_L	-	Panel length factor for average oil rise calculations
Δh	m	Height of radiator center above winding center: assumed thermal head for ONAN
$\Delta\theta_{co}$	K	Top oil temperature rise above average oil
$\Delta\theta_{topoil}$	K	Top oil temperature rise above ambient

Moreover, it is beneficial to understand the ONAN-cooling mode and how the radiators of a transformer are sized. In the presence of a temperature difference, a loop is created by two columns of oil. The column with a higher density experiences greater pressure at its bottom, causing a flow towards the bottom of the column with lower density. This flow continues until the pressure in both columns equalizes. In “ON”-cooled transformers, the warm oil in the tank circulates through the cooler using a mechanism called “thermosyphonic” oil circulation. This circulation is continuous as long as there is a heat source and heat sink, maintaining a pressure imbalance and ensuring a continuous flow of liquid. In an ONAN transformer, heat produced in the core and windings is conducted to the oil, circulated throughout the circuit by thermosyphonic convection, and dissipated to the surrounding air through natural convection, as depicted in Figure A2.

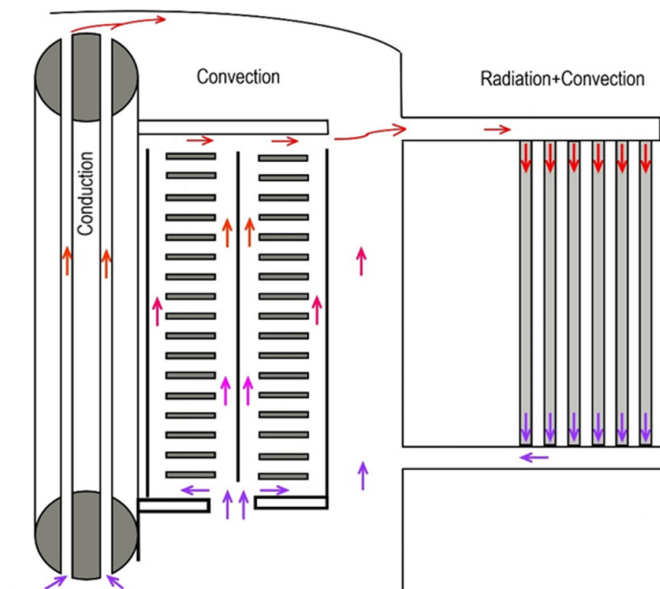


Figure A2. ONAN cooling diagram.

References

1. Radakovic, Z.; Feser, K. A new method for the calculation of the hot-spot temperature in power transformers with ONAN cooling. *IEEE Trans. Power Deliv.* **2003**, *18*, 1284–1292. [[CrossRef](#)]
2. Paramane, S.B.; Joshi, K.; Van Der Veken, W.; Sharma, A. CFD study on thermal performance of radiators in a power transformer: Effect of blowing direction and offset of fans. *IEEE Trans. Power Deliv.* **2014**, *29*, 2596–2604. [[CrossRef](#)]
3. Wu, T.; Yang, F.; Farooq, U.; Jiang, J.; Hu, X. Real-time calculation method of transformer winding temperature field based on sparse sensor placement. *Case Stud. Therm. Eng.* **2023**, *47*, 103090. [[CrossRef](#)]
4. Torriano, F.; Chaaban, M.; Picher, P. Numerical study of parameters affecting the temperature distribution in a disc-type transformer winding. *Appl. Therm. Eng.* **2010**, *30*, 2034–2044. [[CrossRef](#)]
5. Taghikhani, M.A.; Gholami, A. Prediction of hottest spot temperature in power transformer windings with non-directed and directed oil-forced cooling. *Int. J. Electr. Power Energy Syst.* **2009**, *31*, 356–364. [[CrossRef](#)]
6. Gastelurrutia, J.; Ramos, J.C.; Larraona, G.S.; Rivas, A.; Izagirre, J.; Del Río, L. Numerical modelling of natural convection of oil inside distribution transformers. *Appl. Therm. Eng.* **2011**, *31*, 493–505. [[CrossRef](#)]
7. Li, X.K.; Massarotti, N.; Nithiarasu, P.; Fdhila, R.B.; Kranenborg, J.; Laneryd, T.; Olsson, C.-O.; Samuelsson, B.; Gustafsson, A.; Lundin, L.-Å. Thermal modeling of power transformer radiators using a porous medium based CFD approach. In Proceedings of the Second International Conference on Computational Methods for Thermal Problems, Dalian, China, 5–7 September 2011.
8. Kim, M.G.; Cho, S.M.; Kim, J.K. Prediction and evaluation of the cooling performance of radiators used in oil-filled power transformer applications with non-direct and direct-oil-forced flow. *Exp. Therm. Fluid. Sci.* **2013**, *44*, 392–397. [[CrossRef](#)]
9. Cha, C.H.; Kim, J.K.; Kweon, K.Y. Investigation of the thermal head effect in a power transformer. In Proceedings of the Transmission & Distribution Conference & Exposition: Asia and Pacific, Seoul, Republic of Korea, 26–30 October 2009; pp. 1–4. [[CrossRef](#)]
10. Țălu, Ș.D.L.; Țălu, M.D.L. Dimensional Optimization of Frontal Radiators of Cooling System for Power Transformer 630 kVA 20/0.4 kV in Terms of Maximum Heat Transfer. 2010. Available online: https://www.researchgate.net/publication/268436870-Dimensional_optimization_of_frontal_radiators_of_cooling_system_for_power_transformer_630_kVA_2004_kV_in_terms_of_maximum_heat_transfer (accessed on 27 July 2023).
11. Seong, J.K.; Choi, M.J.; Woo, S.G.; Baek, B.S.; Hur, S.J. Evaluation of the cooling capacity for oil immersed transformer radiator using numerical analysis. In Proceedings of the Korean Society of Mechanical Engineers Autumn Conference, Seoul, Republic of Korea, 4–5 October 2012; pp. 61–65.
12. Dorella, J.J.; Storti, B.A.; Rodriguez, G.A.R.; Storti, M.A. Enhancing heat transfer in power transformer radiators via thermo-fluid dynamic analysis with periodic thermal boundary conditions. *Int. J. Heat. Mass. Transf.* **2024**, *222*, 125142. [[CrossRef](#)]
13. Azbar, N.M.; Jaffal, H.M.; Freegah, B. Enhancement of the Thermal Performance Characteristics of an Electrical Power Transformer. *Eng. Sci. Technol.* **2020**, *1*, 94–112. [[CrossRef](#)]
14. Cho, S.M.; Kim, C.S. Classical approach and CFD Analysis for calculating radiator efficiency for Power Transformer. In Proceedings of the KSME Conference, Jeju, Republic of Korea, 3–5 April 2010; pp. 2733–2738.
15. Shim, H.S.; Lee, S.W.; Kang, H.; Choi, J.U.; Park, S.W.; Lee, J.H. A study of temperature analysis considered characters of power transformer's radiator. In Proceedings of the KIEE Conference, Seoul, Republic of Korea, 20–22 October 2011; pp. 118–120.
16. Nabati, H.; Mahmoudi, J.; Ehteram, A. Heat Transfer and Fluid Flow Analysis of Power Transformer's Cooling System Using CFD Approach. *Chem. Prod. Process Model.* **2009**, *4*. [[CrossRef](#)]
17. Rodriguez, G.R.; Garelli, L.; Storti, M.; Granata, D.; Amadei, M.; Rossetti, M. Numerical and experimental thermo-fluid dynamic analysis of a power transformer working in ONAN mode. *Appl. Therm. Eng.* **2017**, *112*, 1271–1280. [[CrossRef](#)]
18. Van Der Veken, W.; Paramane, S.B.; Mertens, R.; Chandak, V.; Coddé, J. Increased Efficiency of Thermal Calculations via the Development of a Full Thermohydraulic Radiator Model. *IEEE Trans. Power Deliv.* **2016**, *31*, 1473–1481. [[CrossRef](#)]
19. Chandak, V.; Paramane, S.B.; Veken, W.V.D.; Codde, J. Numerical investigation to study effect of radiation on thermal performance of radiator for ONAN cooling configuration of transformer. In Proceedings of the IOP Conference Series Materials Science and Engineering, Selangor, Malaysia, 21–23 November 2015. [[CrossRef](#)]
20. Paramane, S.B.; Van Der Veken, W.; Sharma, A.; Coddé, J. Effect of fan arrangement and air flow direction on thermal performance of radiators in a power transformer. *J. Power Technol.* **2017**, *97*, 127–134.
21. Medeiros, L.H.; Oliveira, M.M.; Beltrame, R.C.; Bender, V.C.; Marchesan, T.B.; Marin, M.A. Thermal Experimental Evaluation of a Power Transformer Under OD/OF/ON Cooling Conditions. In Proceedings of the 2023 15th Seminar on Power Electronics and Control, SEPOC 2023, Santa Maria, Brazil, 22–25 October 2023. [[CrossRef](#)]
22. Rodrigues, T.F.; Medeiros, L.H.; Oliveira, M.M.; Nogueira, G.C.; Bender, V.C.; Marchesan, T.B.; Falcao, C.E.G.; Marin, M.A. Evaluation of Power Transformer Thermal Performance and Optical Sensor Positioning Using CFD Simulations and Temperature Rise Test. *IEEE Trans. Instrum. Meas.* **2023**, *72*, 7002511. [[CrossRef](#)]
23. Raeisian, L.; Niazmand, H.; Ebrahimi-Bajestan, E.; Werle, P. Thermal management of a distribution transformer: An optimization study of the cooling system using CFD and response surface methodology. *Int. J. Electr. Power Energy Syst.* **2019**, *104*, 443–455. [[CrossRef](#)]
24. Amoiralis, E.I.; Georgilakis, P.S.; Tsili, M.A.; Kladas, A.G. Global transformer optimization method using evolutionary design and numerical field computation. *IEEE Trans. Magn.* **2009**, *45*, 1720–1723. [[CrossRef](#)]

25. Anishek, S.; Sony, R.; Kumar, J.J.; Kamath, P.M. Performance Analysis and Optimisation of an Oil Natural Air Natural Power Transformer Radiator. *Procedia Technol.* **2016**, *24*, 428–435. [CrossRef]
26. Smolka, J. CFD-based 3-D optimization of the mutual coil configuration for the effective cooling of an electrical transformer. *Appl. Therm. Eng.* **2013**, *50*, 124–133. [CrossRef]
27. El Wakil, N.; Chereches, N.-C.; Padet, J. Numerical study of heat transfer and fluid flow in a power transformer. *Int. J. Therm. Sci.* **2006**, *45*, 615–626. [CrossRef]
28. Chereches, N.C.; Chereches, M.; Miron, L.; Hudisteanu, S. Numerical Study of Cooling Solutions Inside a Power Transformer. *Energy Procedia* **2017**, *112*, 314–321. [CrossRef]
29. Nematzadeh, N.; Ghaebi, H.; Aghdam, E.A. Thermo-Economic Analysis of Innovative Integrated Power Cycles for Low-Temperature Heat Sources Based on Heat Transformer. *Sustainability* **2022**, *14*, 13194. [CrossRef]
30. Eslamian, M.; Vahidi, B.; Eslamian, A. Thermal analysis of cast-resin dry-type transformers. *Energy Convers. Manag.* **2011**, *52*, 2479–2488. [CrossRef]
31. ANSYS FLUENT Theory Guide. Available online: https://www.afs.enea.it/project/neptunius/docs/fluent/html/th/main_pre.htm (accessed on 27 July 2023).
32. Koca, A.; Çalışkan, C.İ.; Koç, E.; Akbal, Ö. A Novel 3D Printed Air-Cooled Fuel Cooler Heat Exchanger for Aviation Industry. *Heat. Transf. Eng.* **2023**, *44*, 1350–1371. [CrossRef]
33. Menter, F.R. Two-equation eddy-viscosity turbulence models for engineering applications. *AIAA J.* **1994**, *32*, 1598–1605. [CrossRef]
34. Awad, O.I.; Mamat, R.; Ali, O.M.; Azmi, W.H.; Kadirgama, K.; Yusri, I.M.; Leman, A.M.; Yusaf, T. Response surface methodology (RSM) based multi-objective optimization of fusel oil -gasoline blends at different water content in SI engine. *Energy Convers. Manag.* **2017**, *150*, 222–241. [CrossRef]

Disclaimer/Publisher’s Note: The statements, opinions and data contained in all publications are solely those of the individual author(s) and contributor(s) and not of MDPI and/or the editor(s). MDPI and/or the editor(s) disclaim responsibility for any injury to people or property resulting from any ideas, methods, instructions or products referred to in the content.